

WIND LOADING OF NATIONAL BUREAU OF
STANDARDS BUILDING NUMBER 226

by

J. R. Campbell, Research Fellow,
Department of Civil Engineering

J. E. Cermak, Professor-in-Charge,
Fluid Mechanics Program

for

National Bureau of Standards
Gaithersburg Campus
Gaithersburg, Maryland
under
Contract NBS-273-70

January 1972

Fluid Mechanics Program
Fluid Dynamics and Diffusion Laboratory
Department of Civil Engineering
Colorado State University
Fort Collins, Colorado
80521



U18401 0576265

CER71-72JRC-JEC51

ABSTRACT

In this report the mean pressure distributions were obtained for all angles of attack at 10 degree increments from +90 to -90 degrees from the North. A 1:200 scale model was used and was placed in both uniform and boundary-layer velocity profiles.

The observed pressure coefficients were considerably higher in the uniform flow due to the higher average velocity in the vicinity of the model.

Fluctuating pressures were analyzed for pressure tap number one. The model was rotated on the turntable until the maximum pressure fluctuation was obtained. The fluctuating pressure was then spectrum analyzed for several reference velocities and it was found that the form of the spectral density function is independent of Reynolds number in the range of Reynolds numbers investigated.

ACKNOWLEDGMENTS

This study was supported by the National Bureau of Standards. The suggestions and assistance of Dr. R. D. Marshall were especially helpful. The assistance of Mr. J. A. Garrison in supervising the construction of the model as well as his suggestions in the gathering of data is gratefully acknowledged.

TABLE OF CONTENTS

	<u>Page</u>
ABSTRACT	ii
ACKNOWLEDGMENTS	iii
LIST OF FIGURES	v
LIST OF SYMBOLS	vii
I. INTRODUCTION	1
II. EXPERIMENTAL EQUIPMENT	2
A. Model	2
B. Wind Tunnel	3
C. Turntable	4
III. EXPERIMENTAL TECHNIQUES	5
A. Measurement of the Mean Velocity	5
B. Measurement of the Mean Pressures	6
C. Measurement of the Fluctuating Pressures	8
SUMMARY	11
REFERENCES	13
APPENDIX	14
Equipment List	14

LIST OF FIGURES

<u>Figure</u>		<u>Page</u>
1	Meteorological wind tunnel	15
2	Experimental arrangement in place in meteorological wind tunnel	16
2a	Photograph of model of Building No. 226 (1:200 scale)	17
3	Pressure tap locations and model dimensions	18
4	Pressure tap numbers	19
5	Pressure tap locations and model dimensions	20
6	Pressure tap numbers	21
7	Velocity profile at model location without model in place ($X/H = 0$)	22
8	Velocity profile for $\frac{X}{H} = + 3.10$	23
9	Velocity profile for $\frac{X}{H} = + 4.55$	24
10	Static pressure profile for $\frac{X}{H} = + 4.55$	25
11	Velocity profile for $\frac{X}{H} = + 6.82$	26
12	Static pressure profile for $\frac{X}{H} = + 6.82$	27
13	Velocity profile for $\frac{X}{H} = - 4.94$	28
14	Turntable with model in position	29
15	Block diagram of instrumentation used for measurement of RMS and peak-to-peak pressure fluctuations	30
16	Block diagram of instrumentation used for measurement of mean pressure	31
17	Plan view of relative positions of prototype towers and model velocity survey locations	32
18-27	Drawings of isobars on roof of Building No. 226 measured as	
	$C_p = \frac{P - P_{ref}}{\rho \bar{U}_{ref}^2 / 2}$	for uniform flow . . .33-43

LIST OF FIGURES (Continued)

<u>Figure</u>		<u>Page</u>
28-37	Drawings of isobars on roof of Building No. 226 measured as $C_p = \frac{P - P_{ref}}{\rho \bar{U}_{ref}^2 / 2} \quad \text{for boundary}$ layer flow	44-53
38	Angle-of-attack vs transducer RMS and peak-to-peak output	55
39	Typical output from wave analyzer for $\bar{U}_{ref} =$ 26.2 ft/sec.	56
39a	Typical output from wave analyzer for $\bar{U}_{ref} =$ 26.2 ft/sec.	57
40	Pressure-fluctuation spectra for pressure tap No. 1 at $\alpha = 200^\circ$	58

LIST OF SYMBOLS

<u>Symbol</u>		
$C_{\bar{p}}$	Mean pressure coefficient	$\frac{P - P_{ref}}{\rho \bar{U}_{ref}^2 / 2}$
db	Decibel	
E	Voltage	
f	Frequency (Hertz)	
H	Height of model	
n	Filter bandwidth (Hertz)	
P	Mean pressure	
U	Local mean velocity (ft/sec)	
U_{ref}	Free stream velocity (ft/sec)	
u	Fluctuating component of velocity (ft/sec)	
x	Distance horizontal to boundary along wind-tunnel center line	
z	Distance perpendicular to boundary	
α	Angle of attack of wind measured from the North in a clockwise direction (degrees)	
δ	Boundary-layer thickness	
ρ	Mass density of air (slugs/ft ³)	

I. INTRODUCTION

The study of wind induced loads on structures has recently received much interest in both the field of fluid mechanics and in the field of structural design. This interest is no doubt at least partly due to the desire to predict failure of structural elements caused by wind loading. Also, due to the increased use of plastic limits in the design of structures and because of the increased use of glass in structures, more accurate loading limits are required by structural designers. Another reason for the increased interest is due to the increase in economy allowed by a more efficient design.

Due to the complexities involved with the flow over a sharp-edged object, the velocity, pressure, and hence the magnitudes and directions of the forces on the object may not be determined theoretically even for a uniform velocity approaching the object. For a real flow field, however, the approaching flow structure is complicated by the turbulent gusts superimposed on the planetary boundary layer.

Because of the complex nature of a theoretical approach to the wind loading structures this method is usually abandoned in favor of experimental investigation. However, the experimental technique is not without its problems.

In the experimental method, exact similitude of the features of the flow as well as exact similitude of the prototype structure is difficult to achieve. Because of this, approximate similarity is achieved by taking the most important factors into account and neglecting those of lesser importance.

In regard to the flow itself there are problems involved with the modelling of the atmospheric flow characteristics. The characteristics

of the turbulence as well as the gustiness of the atmospheric flow are difficult to duplicate. At present, the method of analysis is to assume that the flow characteristics of the gusty wind may be thought of as quasi-steady so that the flow in the wind tunnel may be chosen as steady.

A problem involved with the determination of the wind loading on structures, in particular, is that of how important are the dynamic effects of the wind-building interaction. In other words, how important are the effects of the movement of the building on the important flow characteristics such as separation and reattachment which indirectly determine the drag on the structure. For the most part, the buildings modelled at the present are rigid.

The purpose of this study is to investigate the mean pressure distribution and pressure fluctuations on a rigid model of building No. 226 at the NBS campus at Gaithersburg, Maryland. The data from this report are eventually to be compared with those taken from the prototype building so that a critical evaluation of how well the model predicts full-scale data can be made. An Advance Copy of a preliminary form of this report was submitted in March 1971.

II. EXPERIMENTAL EQUIPMENT

A. Model

The model used in this study was a 1:200 scale model constructed by Colorado State University. This model was constructed of "Lucite" and had a removable top for the purpose of changing pressure taps and installing the transducers. A view of the model in place in the wind tunnel is shown in Fig. 2 and 2a and the drawings of the building along with the pressure tap numbering system is shown in Figs. 3-6.

The model was mounted at two locations within the wind tunnel as is shown in Fig. 2. The purpose of this was to determine the effects of the wind-tunnel boundary layer on the pressure distribution about the structure.

The pressure taps were constructed by drilling a hole in the wall of the building with a 1/16" O.D. bit which was joined by drilling another hole from the inside approximately half the thickness of the wall with a 1/8" O.D. bit. A small section of brass tubing was then inserted in the larger hole in order to facilitate connection of the tap with the Tygon tubing. The region around the brass tubing was then sealed by means of a plastic compound (Dow Corning 781 silicone rubber sealant).

B. Wind Tunnel

The experimental portions of this study were conducted in the meteorological wind tunnel located in the Fluid Dynamics and Diffusion Laboratory of Colorado State University. The purpose for using this particular wind tunnel was to generate a boundary layer of sufficient thickness to scale to typical thicknesses of the natural boundary layer in the atmosphere. A diagram of the wind tunnel is shown in Fig. 1. In the first 6 ft of the test section, the perimeter of the tunnel is covered with 1/2 in. gravel in order to increase the roughness and thereby fix the boundary-layer transition to a turbulent state. After the roughness elements a triangular shaped fence surrounds the perimeter to further stabilize and thicken the boundary layer. It is possible to remove both the fence and the gravel trips in order to obtain a uniform

velocity profile. This was done in the first portion of the study in order to determine the effects of the boundary-layer thickness relative to building height on the pressure distribution on the model. This also had the effect of decreasing the turbulence level to the same value as that within the boundary layer further downstream. When the model was placed in the uniform flow ($X' = 3$ ft) the boundary-layer thickness was small compared to the building height ($\delta/H < 0.1$) while when the model was submerged in the boundary layer ($X' = 71$ ft) $\delta/H = 4.5$. In the latter position the wave length of longitudinal velocity fluctuation of maximum energy at height H was about 10 cm. A more detailed description of this test facility may be found in the report by Cermak and Plate (1).

C. Turntable

The turntable used for rotating the model is shown in block form in Fig. 14. The 10-turn potentiometer allowed for very accurate determination of the angle of attack of the wind. It was found that angular differences of the order of 0.01 degree could be determined in this manner. However, the absolute values of the angles of attack depended upon a vernier which could be read to within 5 minutes which was approximately the same maximum error obtained in placing the model in position.

The inertia mount is made of concrete and is extremely massive in order to not transmit oscillatory motion from the laboratory floor to the structure. The effects of a dynamic interaction of a model with the wind has not been fully investigated as of yet; however, a rigid model should be satisfactory for Building No. 226 since the structure itself is very rigid.

III. EXPERIMENTAL TECHNIQUES

A. Measurement of the Mean Velocity

The mean velocity was measured by means of a pitot-static probe 1/8 in. in diameter. The tube had four static pressure holes of 0.016 in. in diameter spaced evenly around the circumference of the probe 0.5 in. back from the dynamic tap which was located at the tip of the rounded nose. In the case of the uniform flow, one pitot-static probe was mounted in a fixed position approximately 5 ft behind the end of the contraction in the wind tunnel and 1.5 ft from the ceiling. It was mounted equidistant from either wall in order to insure as little interference as possible from the wall boundary layers. The reference velocity at this point was set at 26.7 ft/sec.

This pitot-static probe then served the dual purpose of acting as the reference for setting the free-stream velocity of the wind tunnel and the static pressure at this point was used as the reference pressure with which to compare the pressure measurements on the model. A similar arrangement was used in the case of the model submersed in the boundary layer of the wind tunnel with the exception that the reference pitot-static probe was placed 5 ft in front of the model to insure as small an interference from the model as possible.

The boundary-layer, mean-velocity survey was taken by means of a pitot static tube attached to a carriage which could be positioned by remote control from outside of the tunnel. The carriage was small enough so that blockage effects on the measurements was minimized, yet it was steady enough that vibration effects were not present.

The mean values of the velocity in the wake of the model were difficult to determine due to the large-scale turbulent fluctuations.

Also, for certain heights within the wake the effects of velocity reversal became prominent. The turbulent pressure fluctuations were damped out by means of a long section of vinyl tubing and the velocity reversal was accounted for by physically reversing the direction of the pitot-static probe. The M.K.S. pressure meter described in the Appendix was used for all pressure measurements.

B. Measurement of the Mean Pressures

The mean pressures on the model were measured by means of 1/16 in. diameter taps drilled into the model and fitted with 1/8 in. diameter copper fittings from within the model. Two-foot sections of 1/8 in. inside diameter tubing connected these fittings to a Scanivalve pressure switch from which a single tube led to the M.K.S. pressure meter described in the Appendix.

The Scanivalve is an instrument which is capable of selecting the pressure input of one piezometer tap from the input of up to 48 taps. It was originally designed for in-flight measurements of the pressure distribution on aircraft. Its use solved many of the problems associated with measuring pressures from a large number of sources. For example, one problem experienced previously was that of effectively blocking the tubes connected to pressure taps not being measured so that jets of air do not exit from the taps not being used to sense the pressure. The Scanivalve closes all pressure lines except the one from which the pressure is being measured. Also by means of the Scanivalve any of the pressure taps could be observed at will by the proper selection of the position of an electrical switch.

The control leads for the Scanivalve as well as the single tube leading from the Scanivalve were run through a hole in the turntable

and connected to the M.K.S. pressure meter. Once the system was installed it was possible to make the measurements corresponding to the various angles of attack and for the 40 pressure taps on the roof, from beneath the wind tunnel where the turntable was located. A diagram of the setup is shown in Fig. 14.

The free-stream velocity of the air was 26.7 ft/sec when the pressures were being measured. The pressure which was used as a reference with which to compare the pressures on the model was chosen as the static pressure in the free stream. This was found to be more constant than that within the boundary layer.

The effect of the Reynolds number on the pressure distribution was assumed to be negligible as is usually the case with sharp-edged structures. This is generally due to the fact that the points of separation of the flow from a sharp-edged object are usually constant. An experimental verification of this assumption is given in the report by Marshall (2) for the Bank of America World Headquarters model.

Figures 18 through 27 on pages 34 through 43 are for the lines of constant C_p when the model was in the uniform flow of 26.7 ft/sec. The boundary-layer thickness at this location ($X' = 3$ ft, $X = 0$) was less than 0.1 H. The dimensionless ratio C_p has the following definition:

$$C_p = \frac{P - P_{ref}}{\rho \bar{U}_{ref}^2 / 2}$$

where P = average surface pressure,

P_{ref} = static pressure at the reference height,

ρ = mass density of air,

and \bar{U}_{ref} = free-stream wind speed.

The static pressure surveys shown in Figs. 10 and 12 were taken in the boundary layer by comparing the static pressure measured on a pitot-static probe attached to the carriage to the static pressure measured by the reference pitot-static probe. The variance of the free-stream static pressure from zero, as is shown by Fig. 12, could possibly be due to either a difference in the characteristic of the pitot-static probes or due to the fact that carriage would not go high enough to show the whole profile.

Figures 28 through 37 on pages 45 through 54 are for the lines of constant C_p for the model placed in the boundary layer 71 ft downstream of the triangular fence. However, it is very easy to see a difference between these and the previous drawings with the model in the uniform stream. In general the values of C_p obtained in the boundary layer are considerably lower than those obtained in the uniform flow.

C. Measurements of the Fluctuating Pressures

The fluctuating components of the pressures on the model were measured by means of a Statham pressure transducer. The transducer was connected to pressure tap No. 1 by approximately 3 in. of 1/8 in. inside diameter Tygon tubing. This length was assumed short enough to prevent damping effects due to the tubing. The reference side of the pressure was found to be stationary enough not to effect the fluctuating portions of the pressure. The static pressure of the reference pitot tube was not used as a reference for the fluctuating pressure measurements due to it being more unstable than the pressure within the model.

measurements due to it being more unstable than the pressure within the model.

The signal from the pressure transducer was amplified by means of a Dana D-C amplifier. The transducer and associated bridge network were powered by a battery as the power supplies tried were too noisy for fluctuating pressure measurement.

The amplified output from the transducer was then monitored simultaneously by a DISA r.m.s. meter as well as an oscilloscope. The turntable was turned 360 degrees and the approximate angle of maximum output was noted. Figure 38 was then constructed in order to determine the exact location of maximum output. The peak-to-peak values were obtained by direct visualization of the trace on the scope whereas the r.m.s. values were obtained by integrating the electrical output from the DISA for approximately 30 sec. This was done to obtain a more accurate reading than by direct observation of the meter since the meter fluctuated wildly in this range of angle-of-attack.

Since 200 degrees turned out to be the angle at which the maximum velocity fluctuation was encountered this angle was chosen as the reference angle used for the spectrum analysis. This direction corresponds to $\alpha = -20^{\circ}$ in the mean pressure coefficient plots where tap No. 1 is reflected in the vertical plane of symmetry passing through the longitudinal axis of the building. For this purpose a General Radio Company Type 1564-A sound and vibration analyzer was used. Following the directions in the manual this produces a record as shown in Fig. 39 when the amplified transducer output is used as an input into the wave analyzer.

The wave analyzer has the advantage that the input and output can be continuously monitored. Therefore, it is possible to determine the distortion imposed on the regular signal by the wave analyzer by switching the filter to all pass and observing the input and output signals on a dual-trace oscilloscope.

The 1/10 octave filter was used in the three runs obtained. In each case the wind-tunnel noise could be determined by adjusting the pitch of the fan blades so that the velocity of the air in the tunnel was zero while the motor itself ran at the same r.p.m.

From Fig. 39 the pressure fluctuation spectra could be determined as shown by Fig. 40. The purpose for this was to qualitatively analyze the effects of free-stream velocity on pressure-fluctuation spectra.

It seems relevant at this point to discuss the procedure by which Fig. 40 was obtained from Fig. 39 as this procedure was not found in the literature. The response in db vs. frequency in Hz was first discretized. The following computational procedure was then followed and the results are presented in Fig. 40:

- 1) f (Hz) was recorded for a particular value as well as the response (db) for that value of f . The response was labeled R for tabulation purpose.
- 2) Next s was defined as $R/20.0$.
- 3) Q was defined as the ratio of E r.m.s./ E r.m.s. min. and was computed from the definition of the decibel as 10^S .
- 4) E r.m.s. (mv) was computed as $Q \cdot E$ r.m.s. min. where E r.m.s. min (mv) was obtained from the dial setting on the band-level switch of the wave analyzer.

- 5) n (Hz) was defined as the bandwidth which for the 1/10 octave bandwidth filter was computed from the formula:

$$n \text{ (Hz)} = \frac{1}{10} [1.5 \cdot f \text{ (Hz)}].$$
 The 1/10 would have been 1/3 in the case of the 1/3 octave band pass filter.
- 6) Finally W was defined as $E \text{ r.m.s./}n$ (mv/Hz).

IV. SUMMARY

One purpose of this study was to provide information to help in locating pressure transducers on the prototype structure which is being instrumented for a full-scale study of wind pressures. A second objective of this study was to obtain wind-pressure data on a small-scale model building which can be used to verify similarity by comparison with data to be obtained on the full-scale building.

Mean-pressure distributions were obtained for all wind directions using a 1:200 scale model of Building No. 226 at the NBS campus at Gaithersburg, Maryland. The measurements were taken in a uniform flow and in a turbulent boundary layer which simulated the atmospheric boundary layer. Distributions of the mean pressure coefficient over the roof surface are shown in Figs. 18-27 for uniform flow and in Figs. 28-34 for the boundary-layer flow.

The mean pressure coefficients measured in the boundary layer were considerably less than those measured in the uniform flow. This is primarily due to the choice of the free stream wind speed as a reference wind speed. The wind-speed distribution through the boundary layer was determined so that the laboratory determined mean pressure coefficients can be readily compared to those which will be determined from prototype measurements.

Vertical distributions of static pressure were measured at the location where the reference pressure was measured. The vertical pressure distributions were taken in order to determine if the building affected the static pressures to be measured in the field.

Exploratory measurements of the pressure fluctuations indicate that the maximum pressure fluctuations for pressure tap No. 1 on the top occur at $\alpha = 200$ degrees (this direction corresponds to $\alpha = -20^\circ$ when tap No. 1 is reflected in a vertical plane of symmetry through the longitudinal axis of the building). This may be seen from Fig. 38.

REFERENCES

1. Cermak, J. E. and Plate, E. J., "Micrometeorological Wind Tunnel Facility, Description and Characteristics," CER63EJP-JEC9, Colorado State University (1963).
2. Marshall, R. D., and Cermak, J. E., "Wind Studies of Bank of America World Headquarters Building," CER66-67RDM-JEC19, Colorado State University (1966).

APPENDIX

Equipment List

Amplifier	Dana Series 3500 Data Amplifiers Gain: 1000 Max. in 6 steps Gain resolution: $\pm 0.01\%$ Input impedance: 10 megohms Output impedance: 100 milliohms Linearity: $\pm 0.01\%$ Frequency response: Rise time: ± 1 db to 20 Khz.
Oscilloscope	Tektronix Type 561A Time Base: Type 67 Amplifier: Type 3A1
Pressure Meter	M.K.S. Baratron Type 77 Electronic Pressure Meter using Type 77H series Pressure Head and Type 77M series Indicators Range: 0.001 mm Hg to 30 mm Hg D.C. output: 100 millivolts full scale.
R.M.S. Meter	Disa Type 55 D35 True R.M.S. Voltmeter Range: 12 full scale ranges from millivolt to 300 volt full scale Frequency response: 1.0 Hz to 400 KHz Input impedance: 1 megohm Time constant: 6 ranges from 0.1 sec. to 3 sec.
Volt Meter	Hewlett Packard Model DY-2401C Integrating Digital Voltmeter Time Constant: 0.01, 0.1, and 1.0 sec. and manual selection Resolution: 1×10^{-6} Volt to 1000 Volt Linearity: $\pm 0.005\%$ Input impedance: 10 megohms
Wave Analyzer	General Radio Company Type 1564-A Sound and Vibration Analyzer Impedance: 6000 ohms Filter Characteristics: 1/10 octave (7%) Range: 2.5 Hz to 25 K Hz in decade ranges

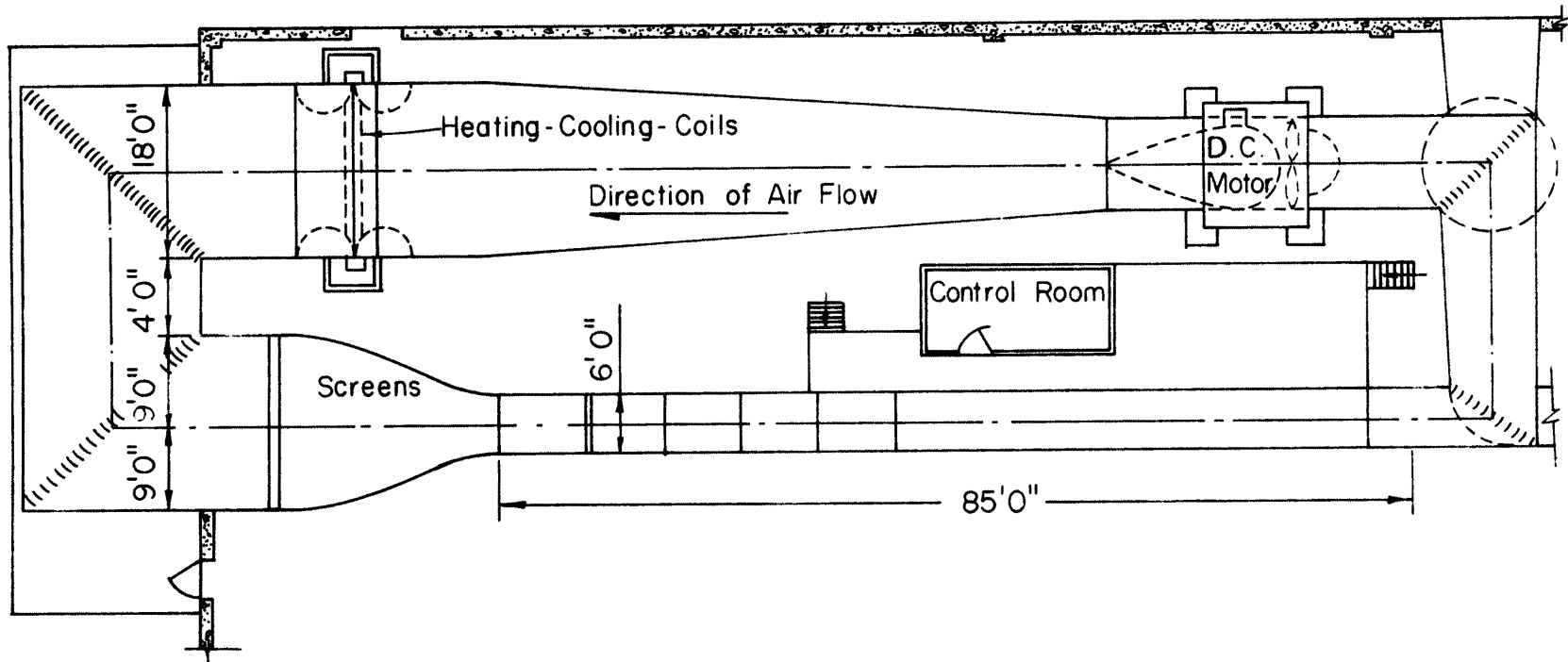
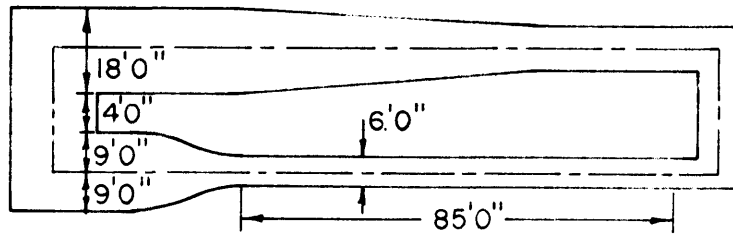
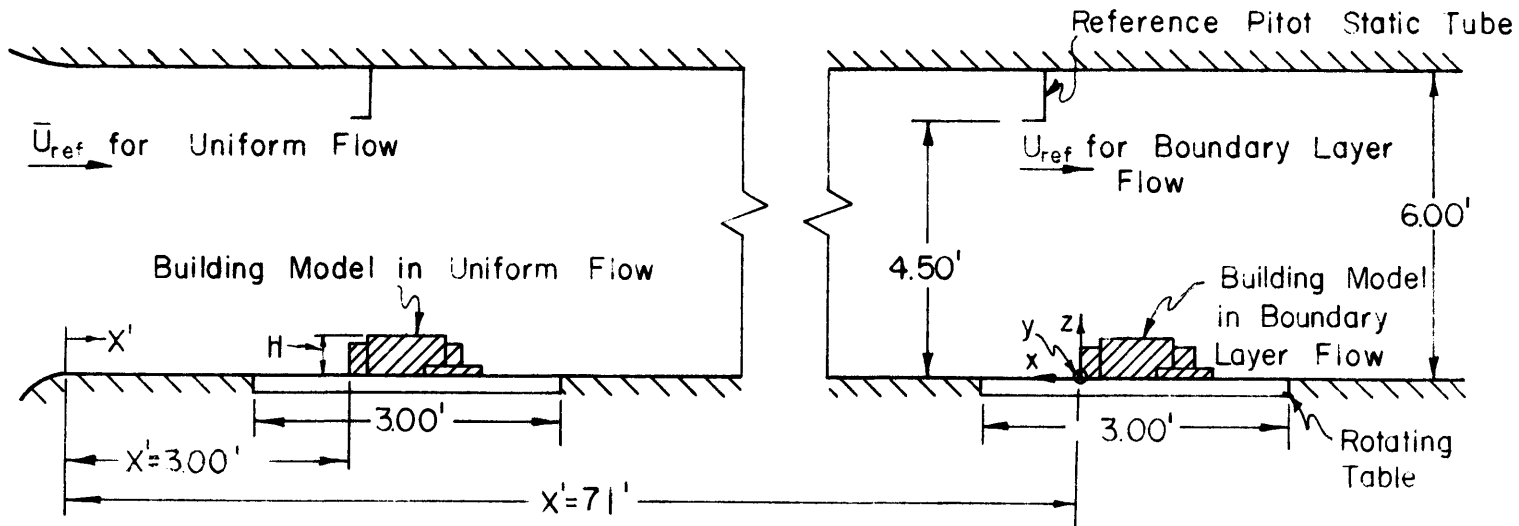


Fig. 1 Meteorological wind tunnel



Top View of Wind Tunnel

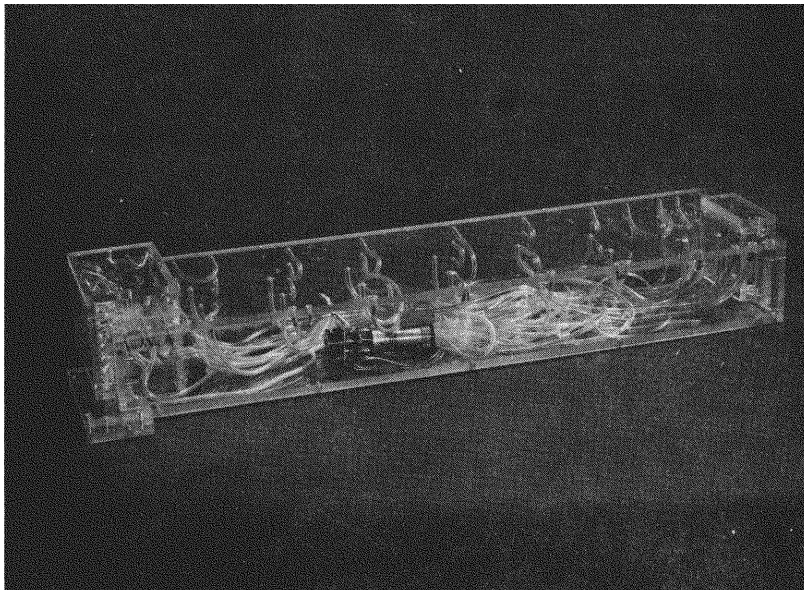


Side View of Working Section

Fig. 2 Experimental arrangement in place in meteorological wind tunnel



Building in Position for Measurements in Uniform Flow (viewed in direction of flow)



Close-up of Building Showing Pressure Taps and Scanivalve

Fig. 2a Photograph of model of Building No. 226 (1:200 scale)

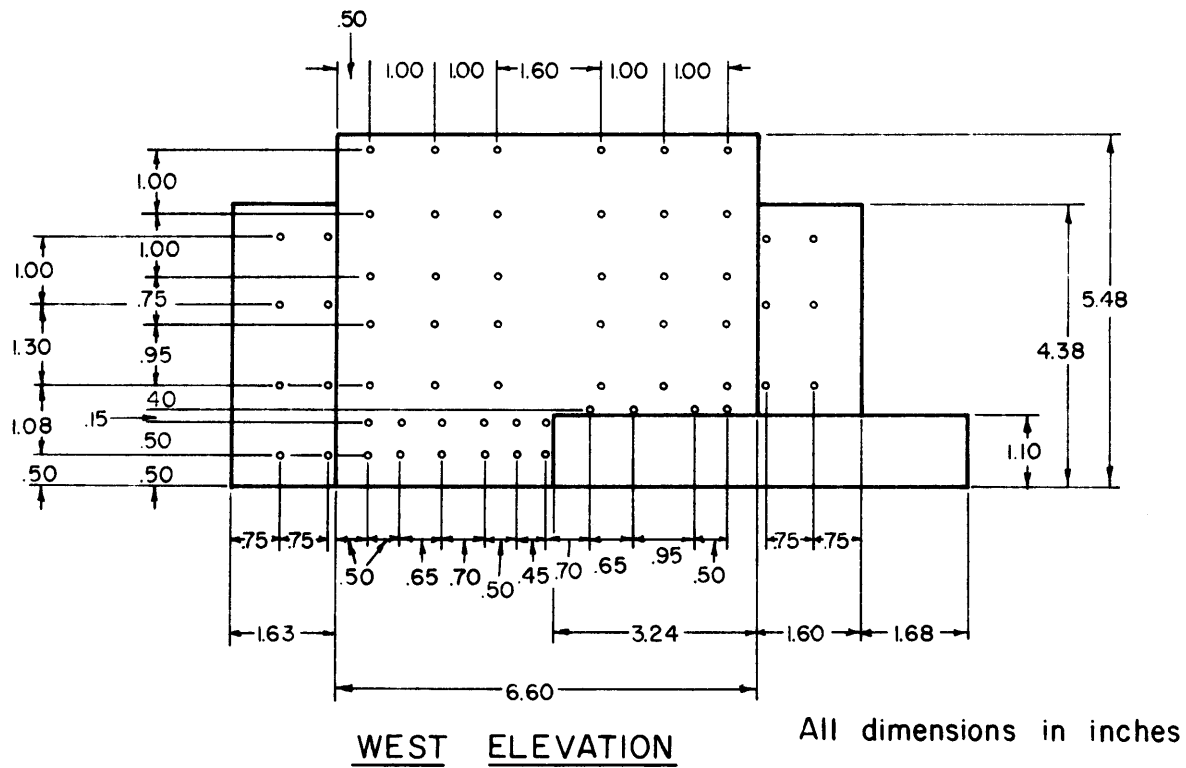
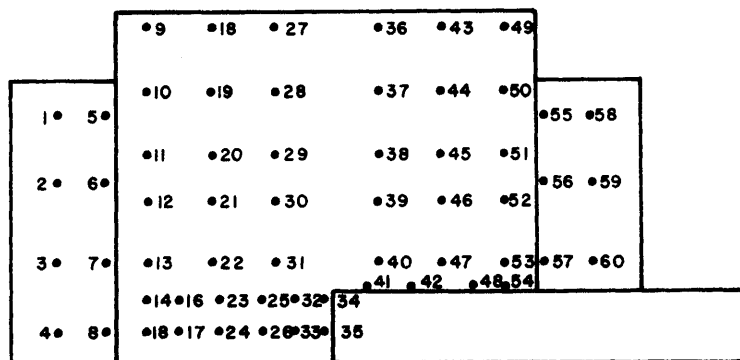
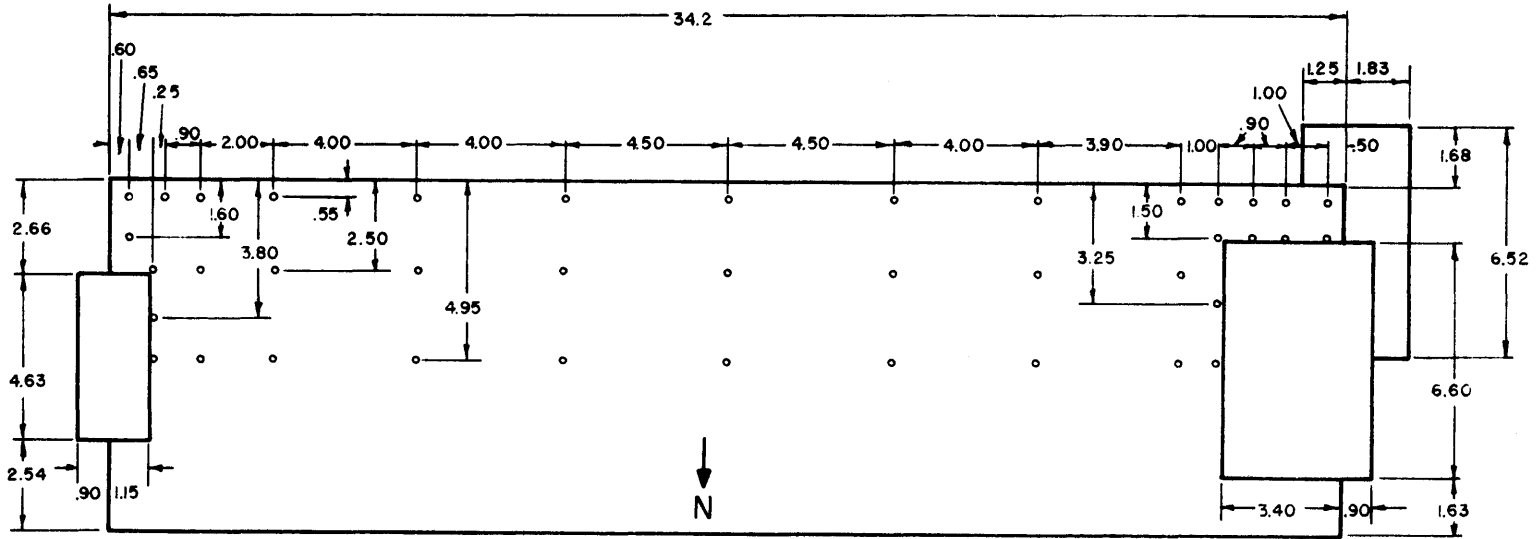


Fig. 3 Pressure tap locations and model dimensions

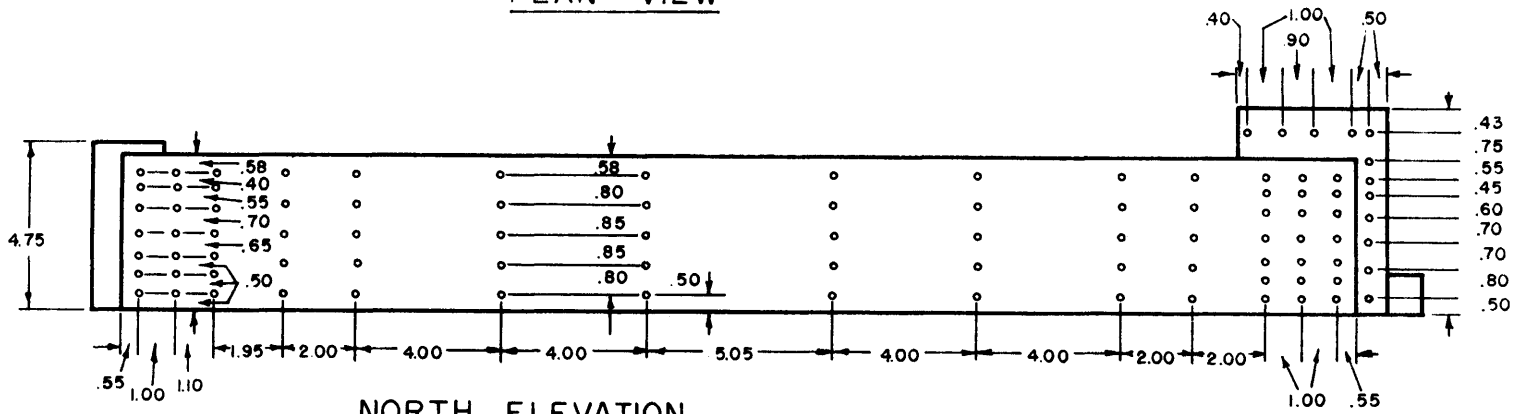


WEST ELEVATION

Fig. 4 Pressure tap numbers



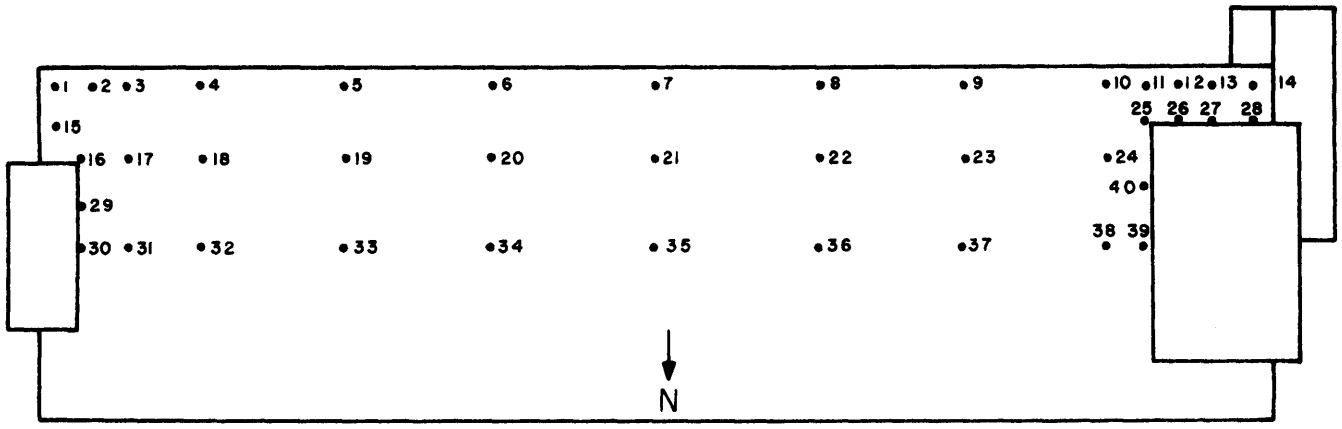
PLAN VIEW



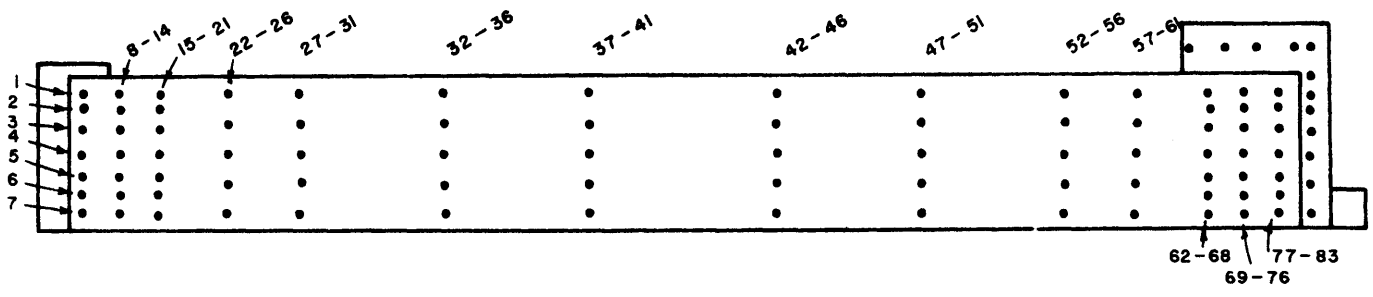
NORTH ELEVATION

All dimensions in inches

Fig. 5 Pressure tap locations and model dimensions



PLAN VIEW



NORTH ELEVATION

Fig. 6 Pressure tap numbers

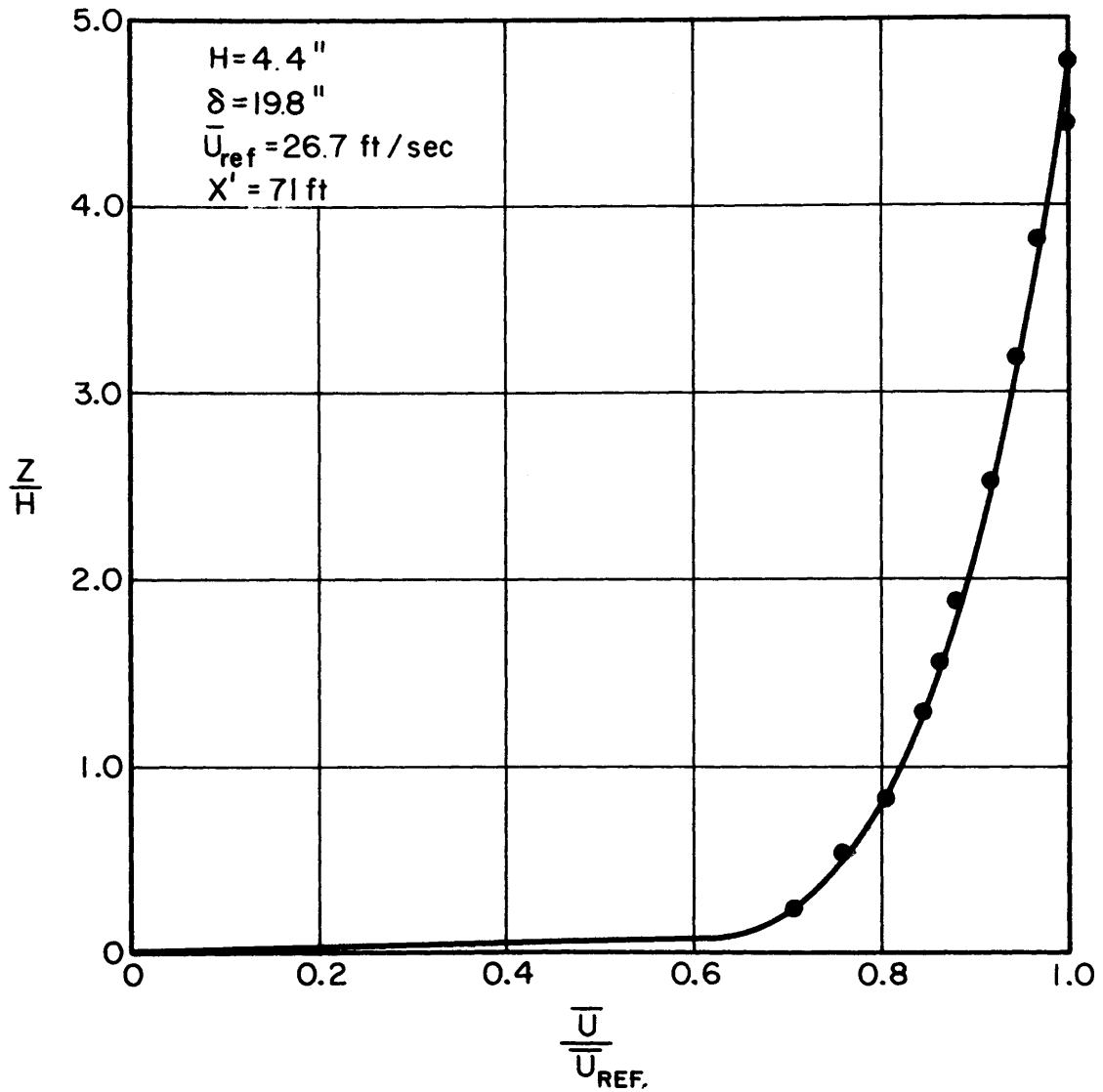


Fig. 7 Velocity profile at model location without model in place ($X/H = 0$)

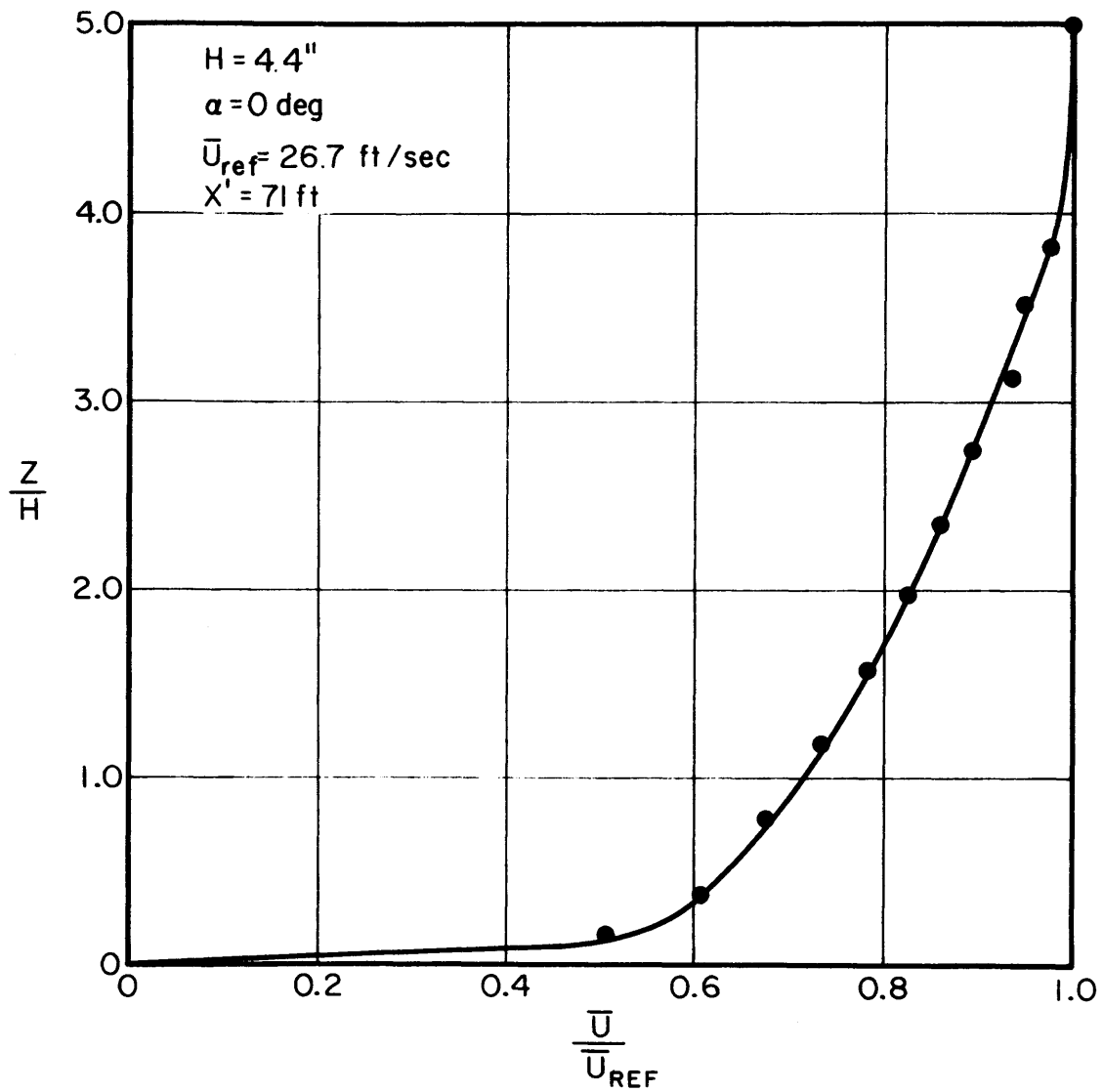


Fig. 8 Velocity profile for $\frac{X}{H} = + 3.1$

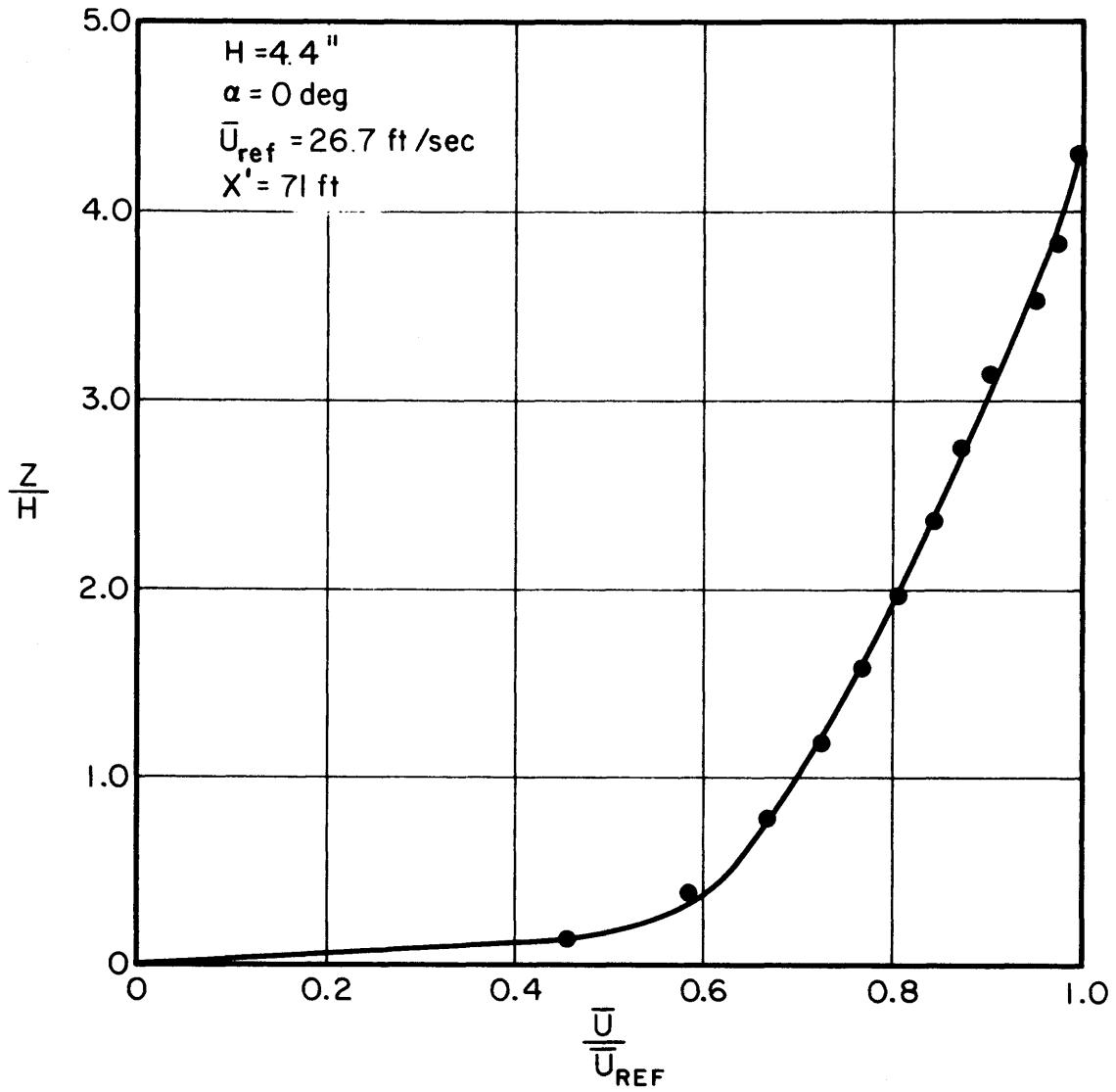


Fig. 9 Velocity profile for $\frac{X}{H} = + 4.55$

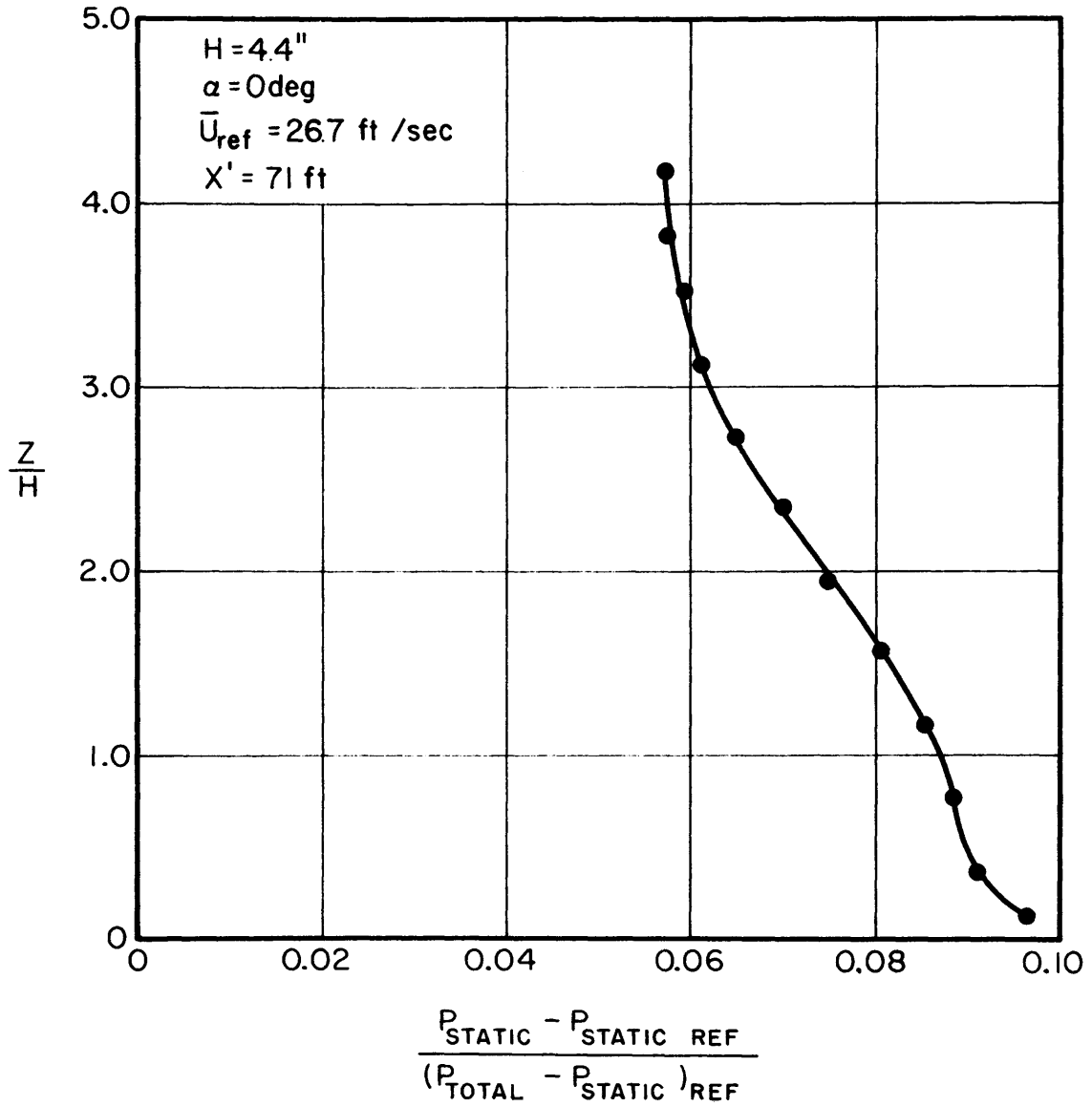


Fig. 10 Static pressure profile for $\frac{X}{H} = + 4.55$

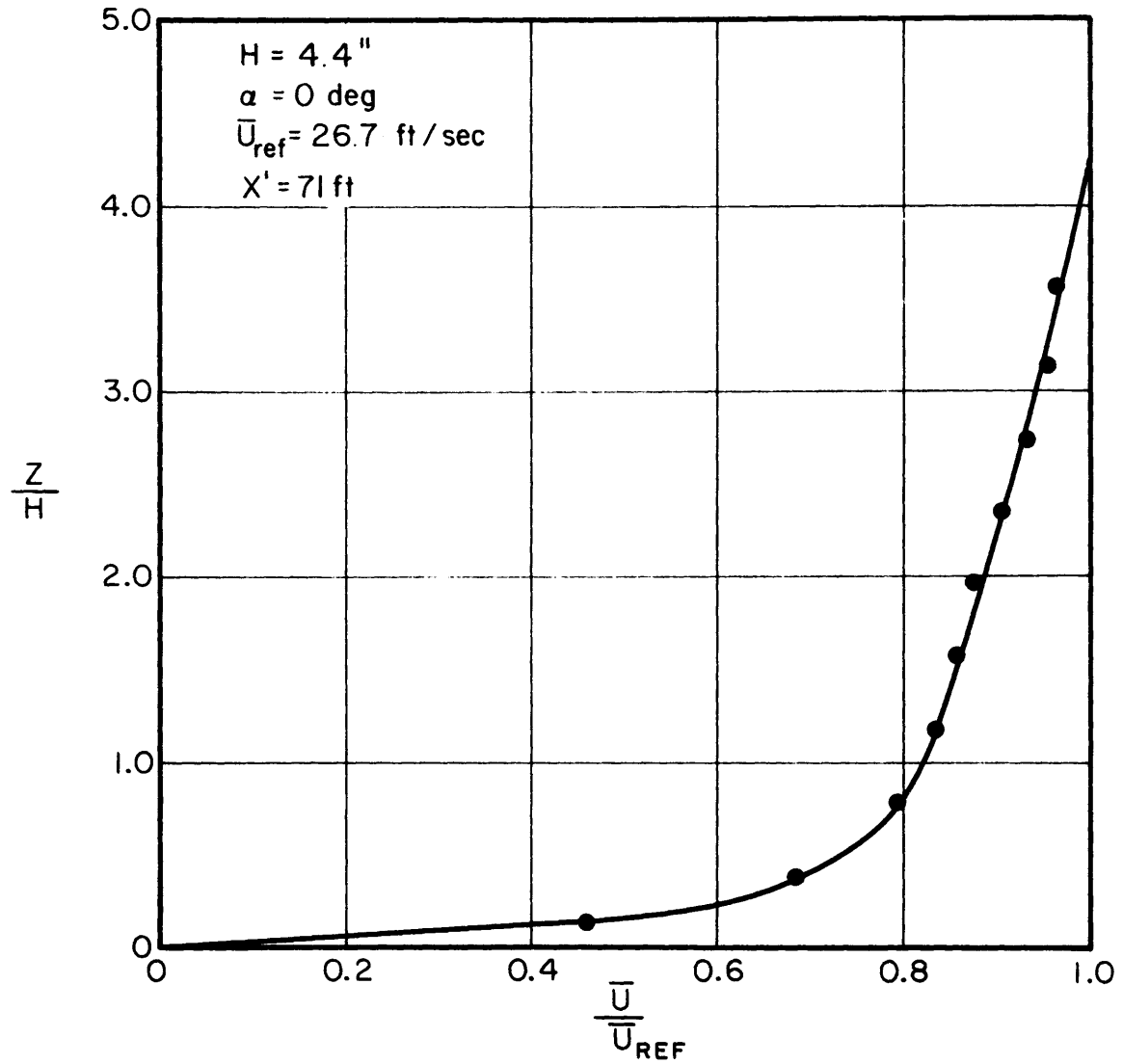


Fig. 11 Velocity profile for $\frac{X}{H} = + 6.82$

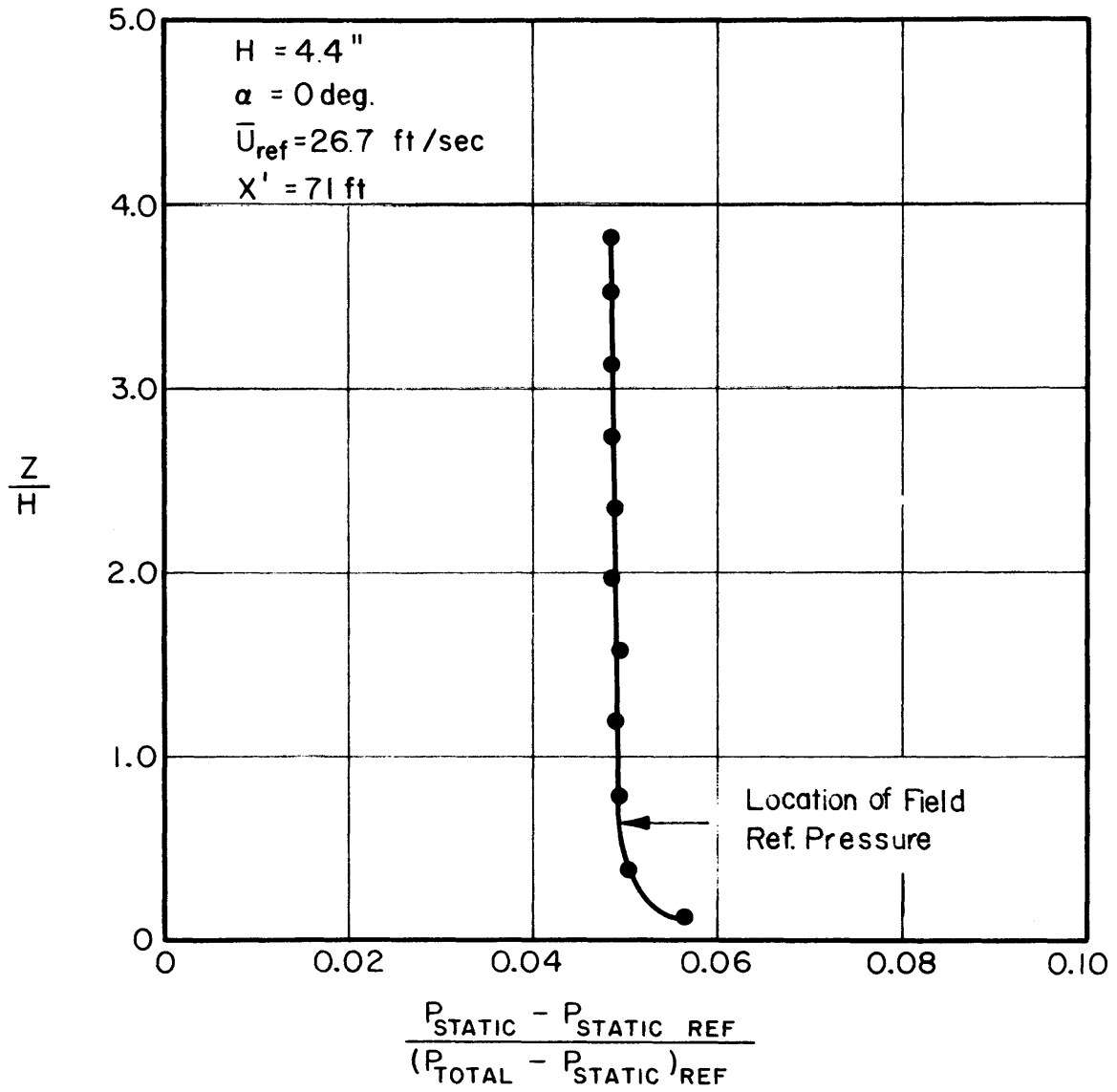


Fig. 12 Static pressure profile for $\frac{X}{H} = + 6.82$

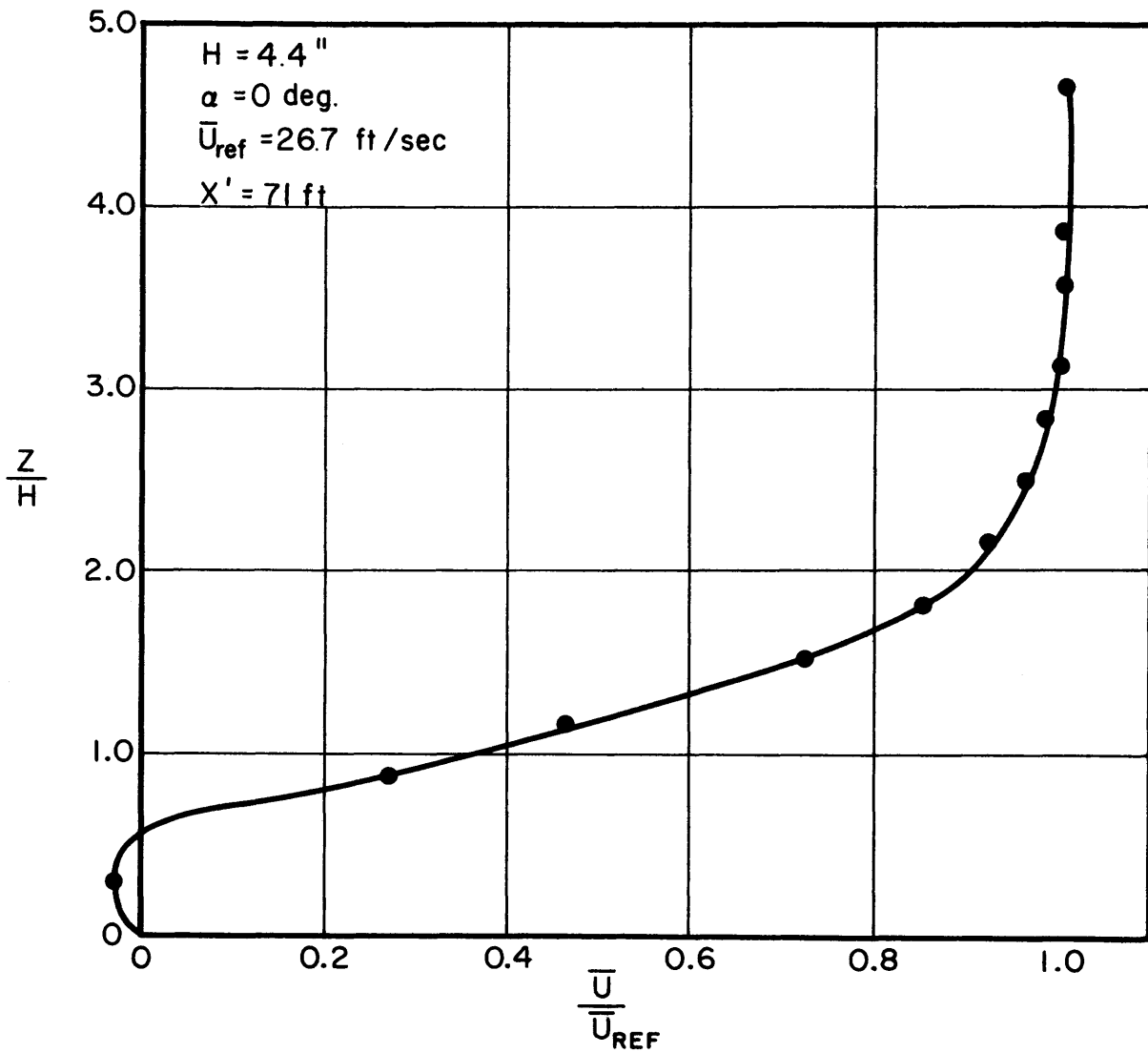


Fig. 13 Velocity profile for $\frac{X}{H} = -4.94$

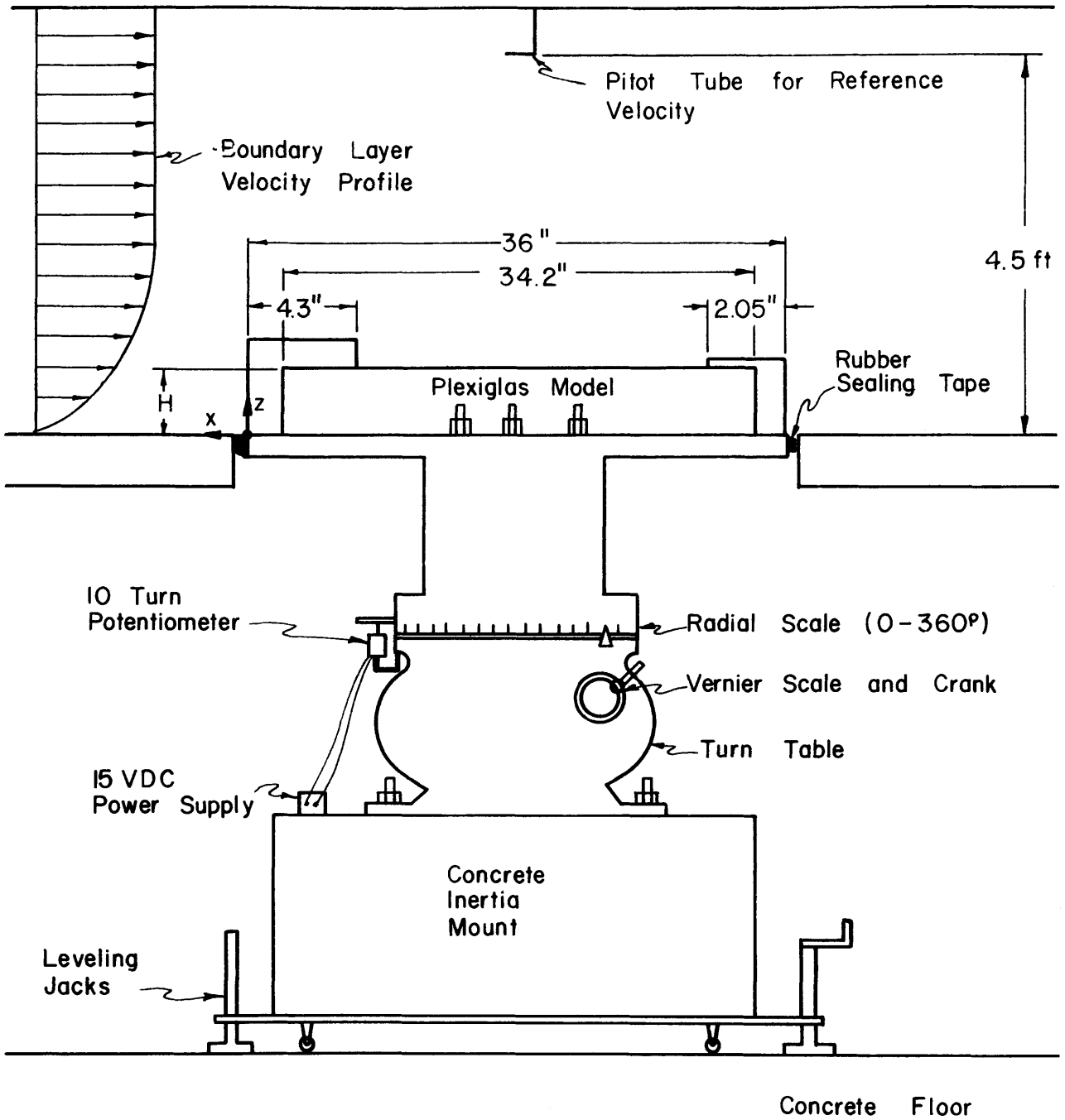


Fig. 14 Turntable with model in position

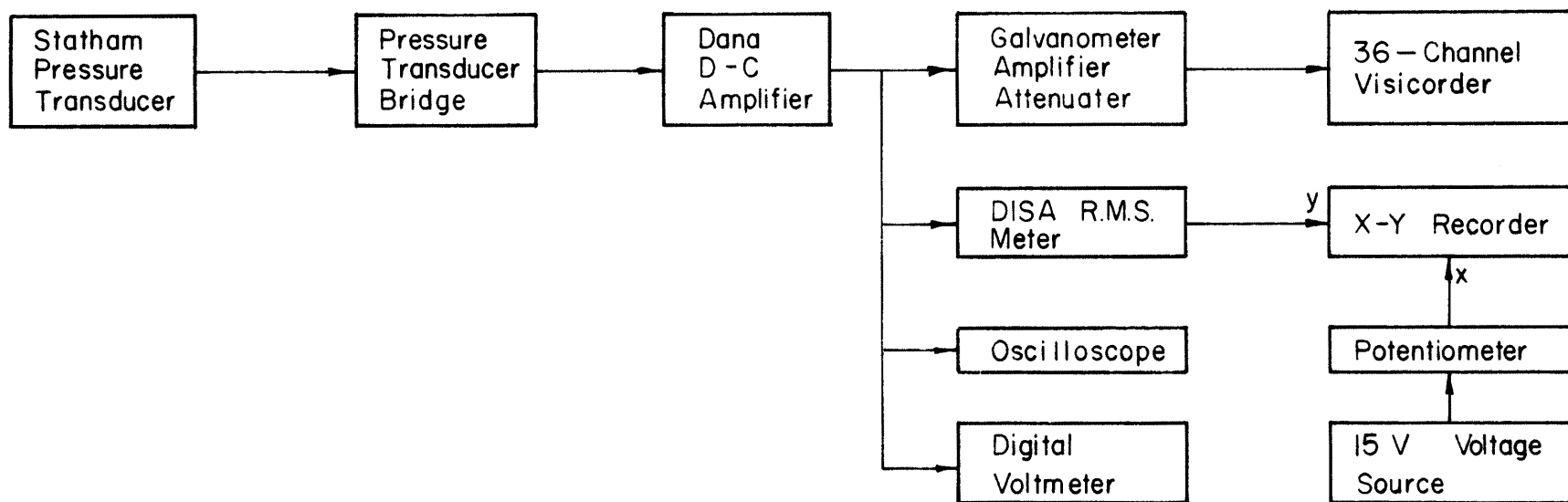


Fig. 15 Block diagram of instrumentation used for measurement of RMS and peak-to-peak pressure fluctuations

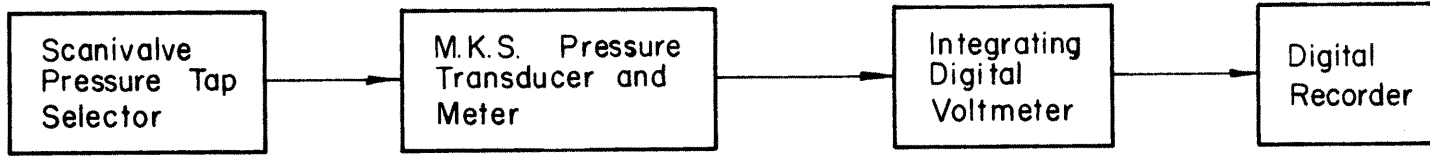


Fig. 16 Block diagram of instrumentation used for measurement of mean pressure

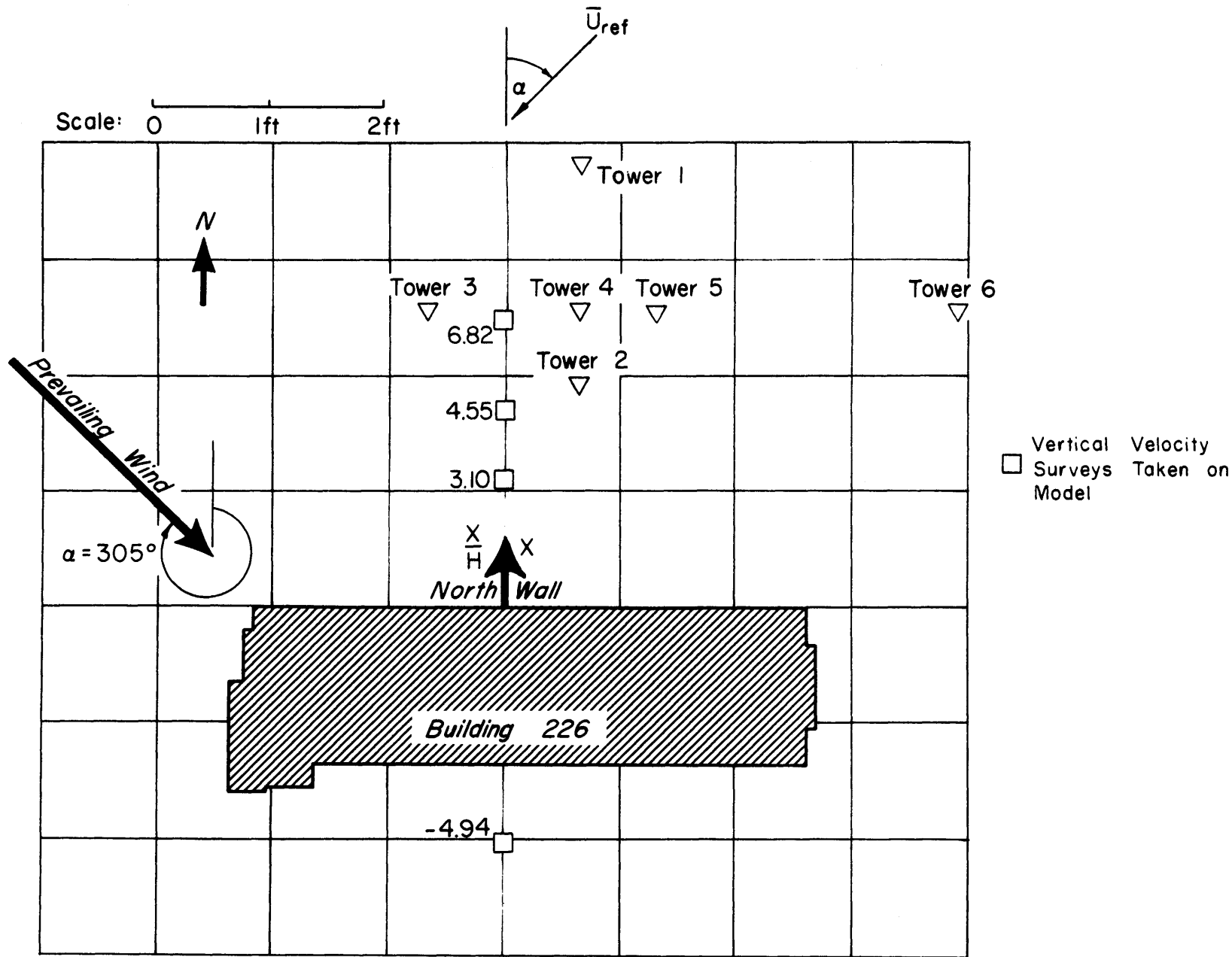


Fig. 17 Plan view of relative positions of prototype towers and model velocity survey locations

Drawings of isobars on roof of Building No. 226 measured as

$$C_p = \frac{P - P_{\text{ref}}}{\rho \bar{U}_{\text{ref}}^2 / 2}$$

For Uniform Flow

Figs. 18-27

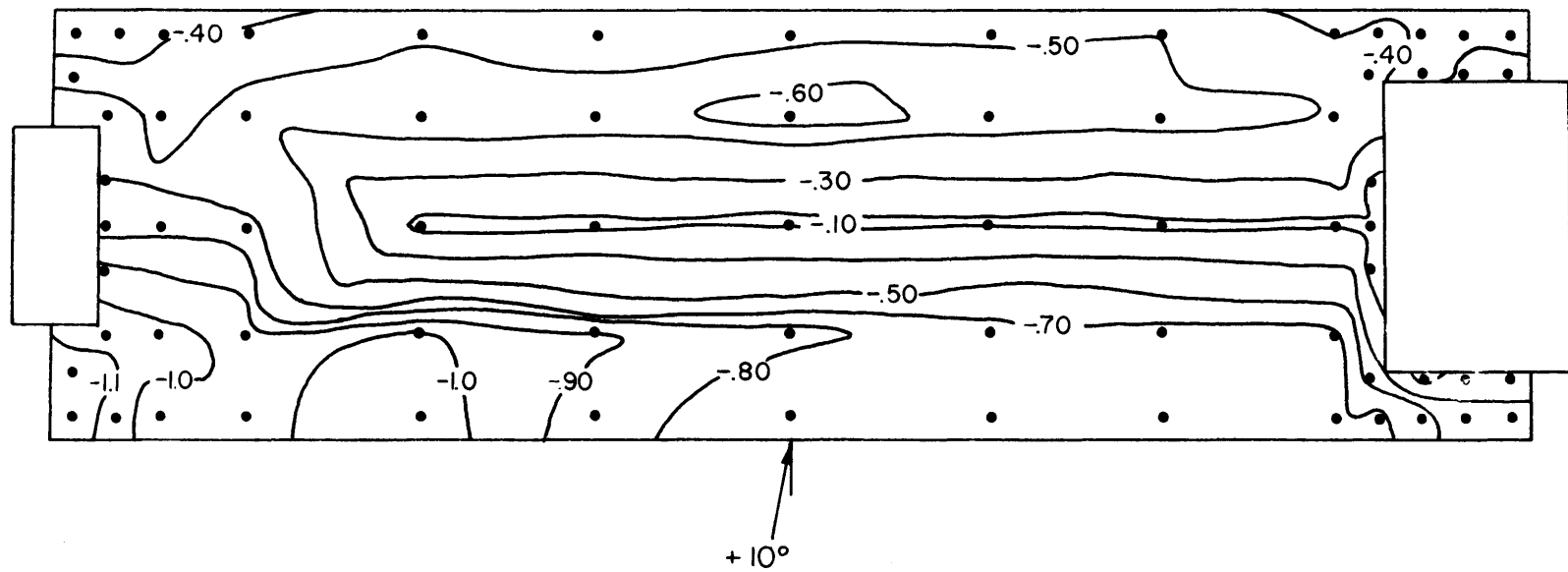
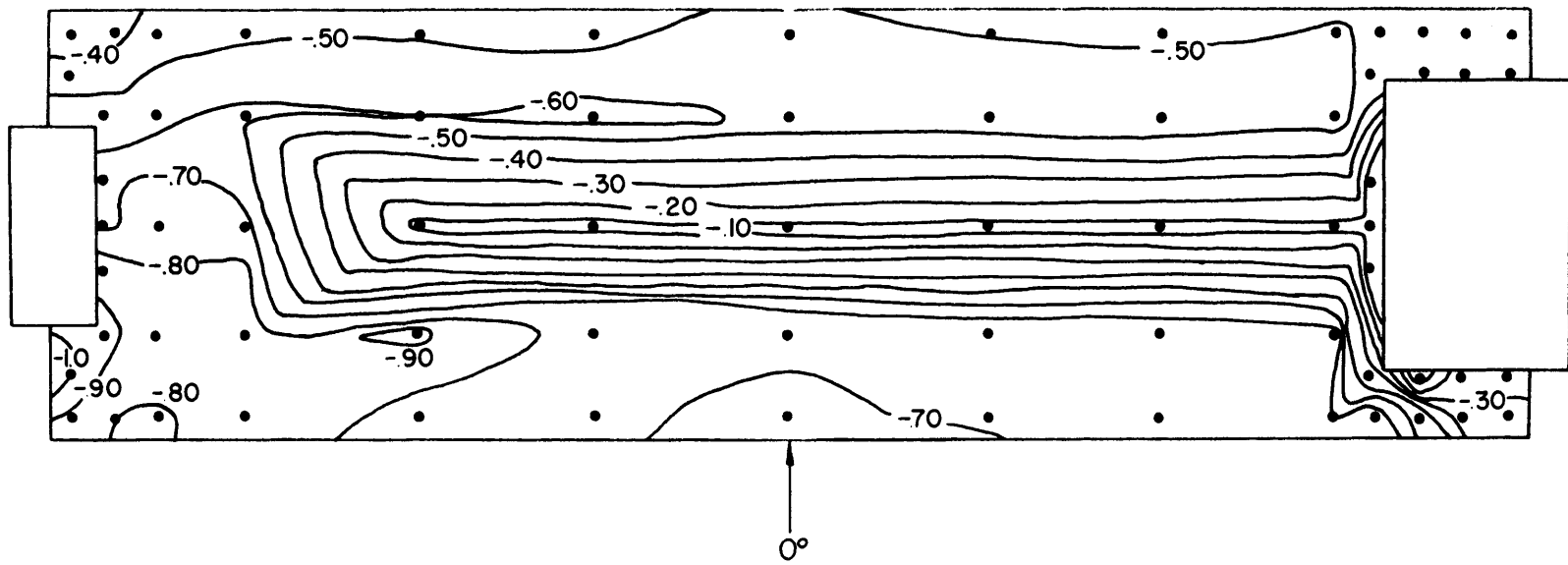


Fig. 18 Mean pressure coefficients for $\alpha = 0^\circ$ and 10° (Uniform Flow)

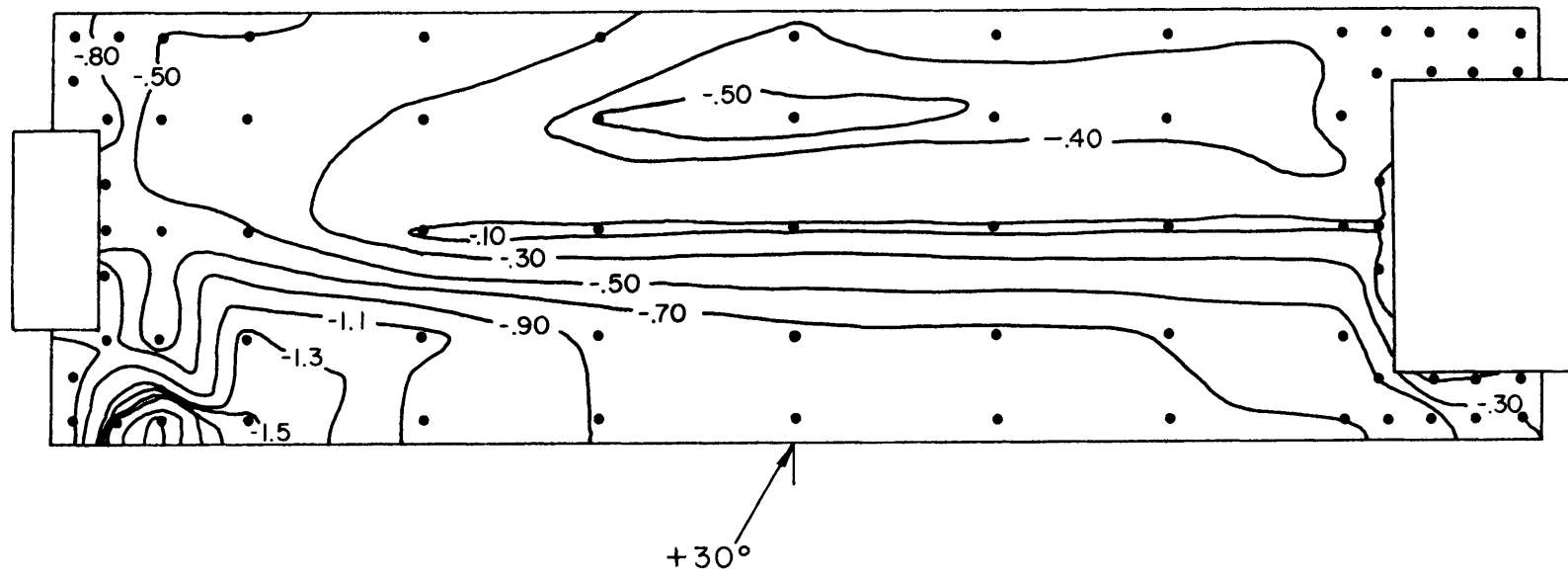
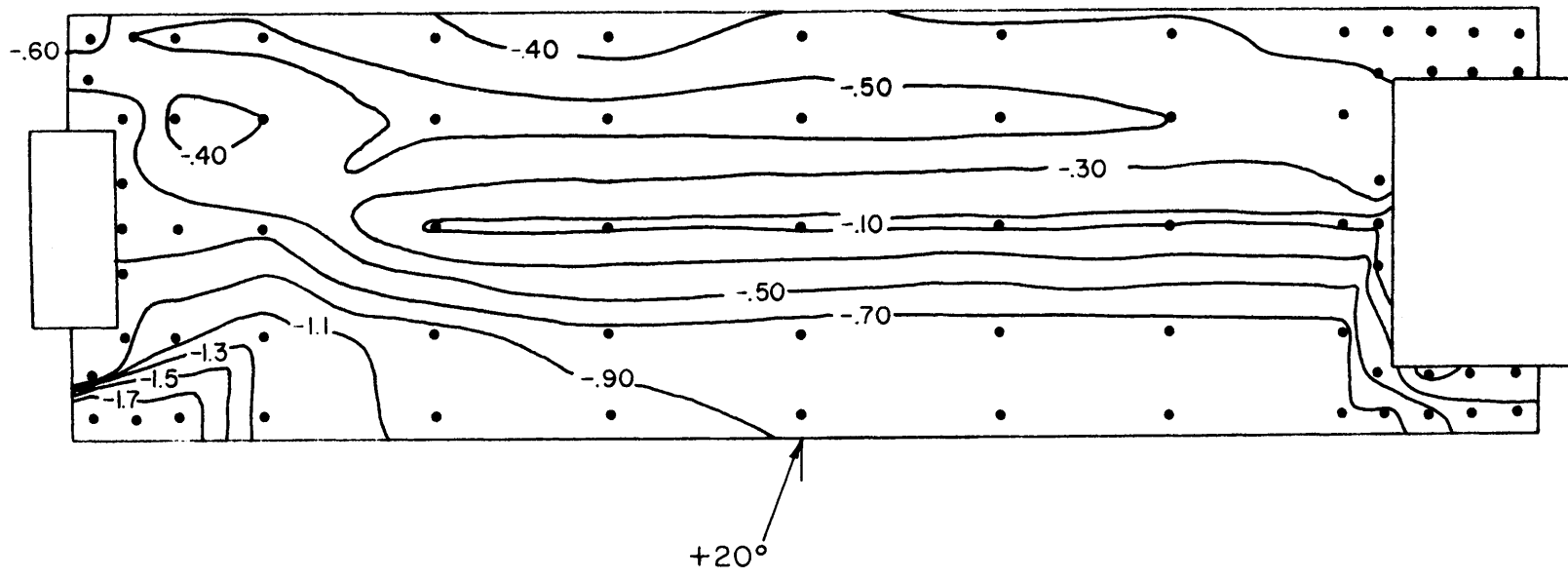


Fig. 19 Mean pressure coefficients for $\alpha = 20^\circ$ and 30° (Uniform Flow)

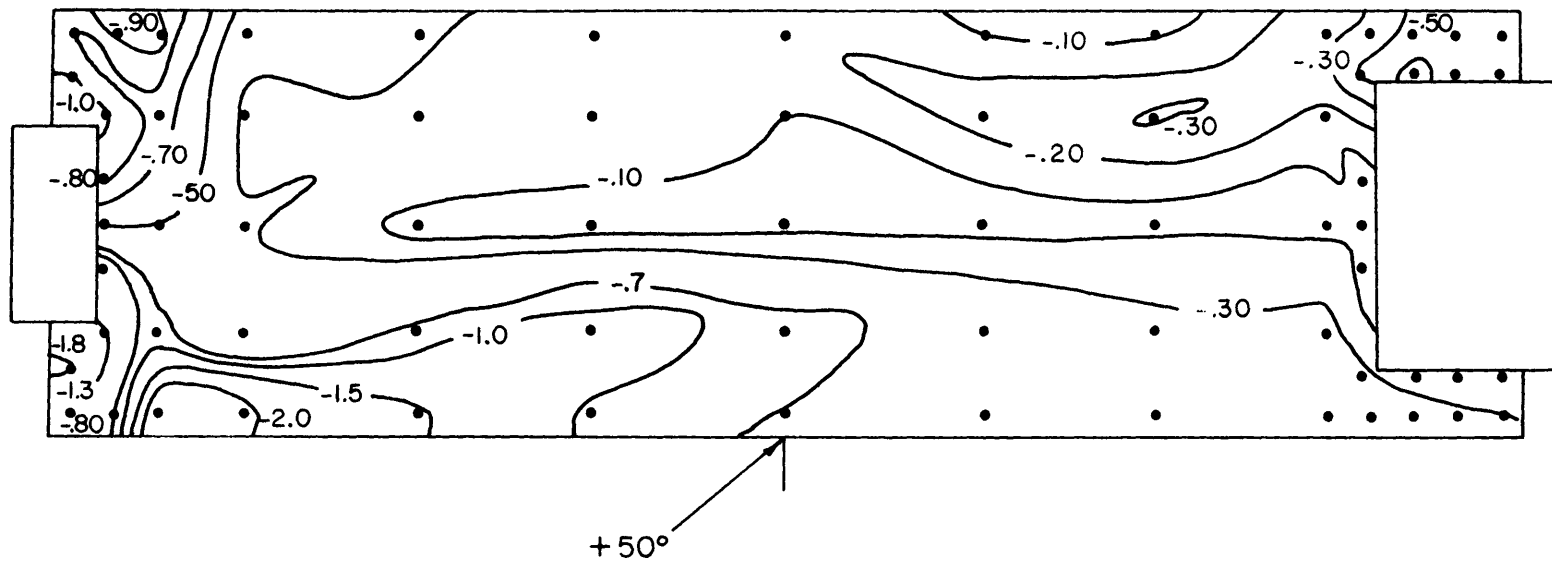
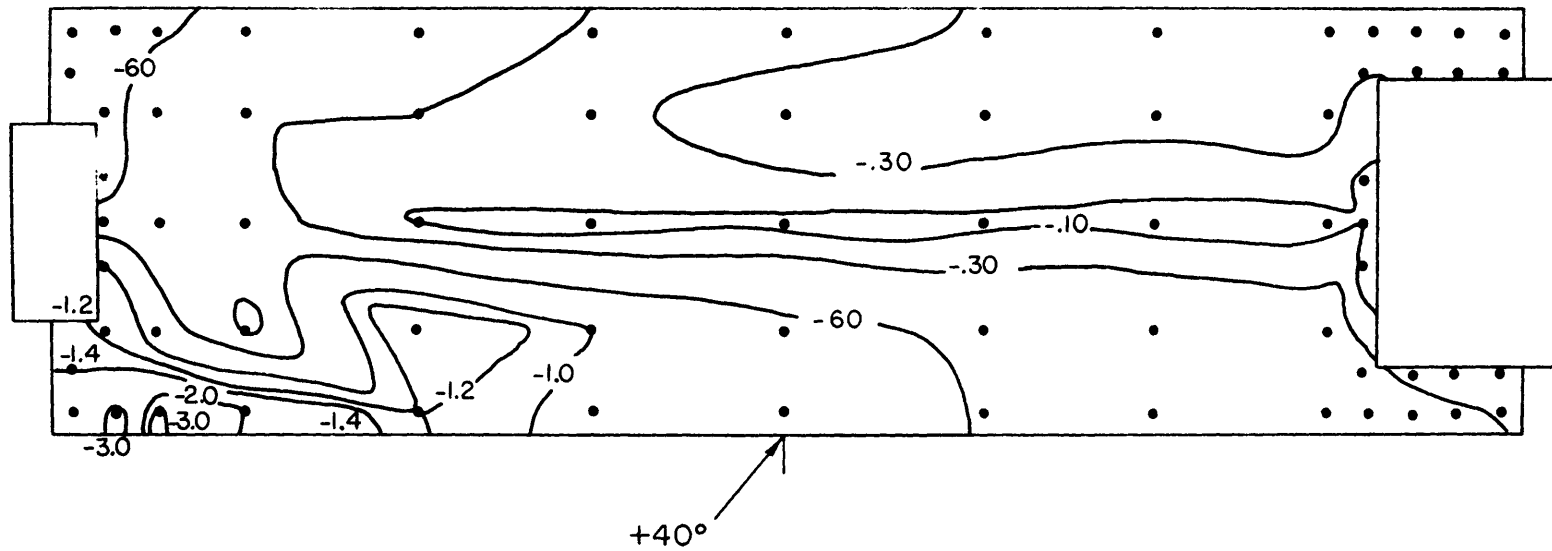


Fig. 20 Mean pressure coefficients for $\alpha = 40^\circ$ and 50° (Uniform Flow)

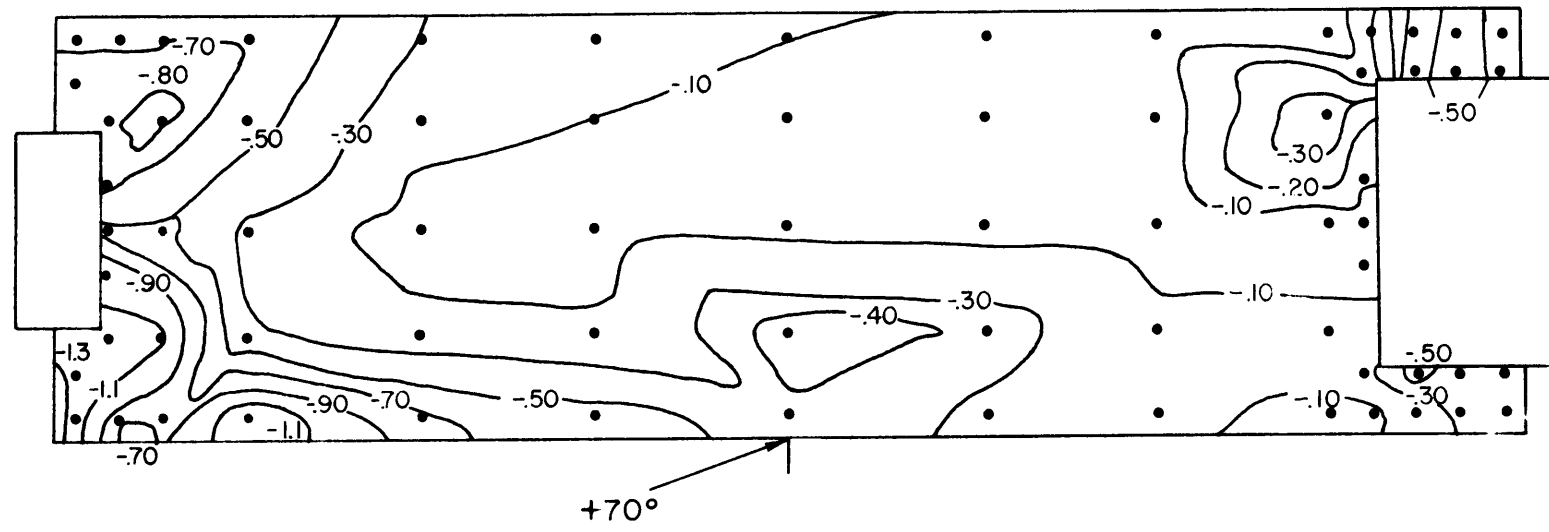
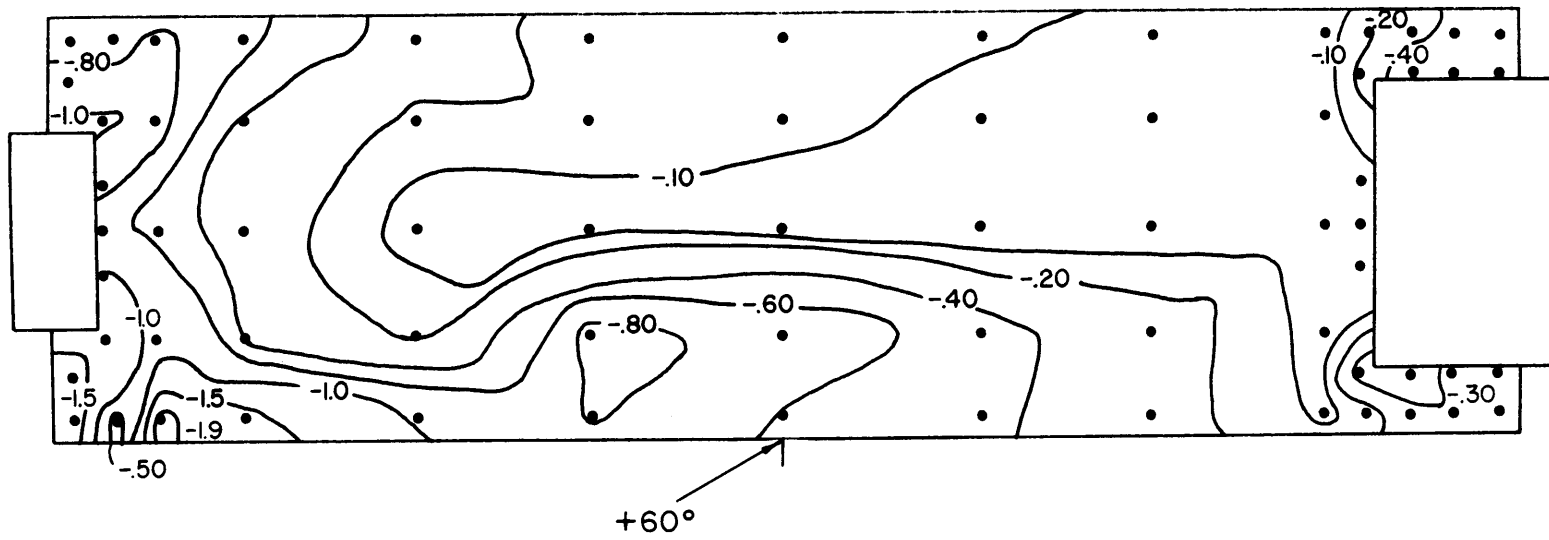


Fig. 21 Mean pressure coefficients for $\alpha = 60^\circ$ and 70° (Uniform Flow)

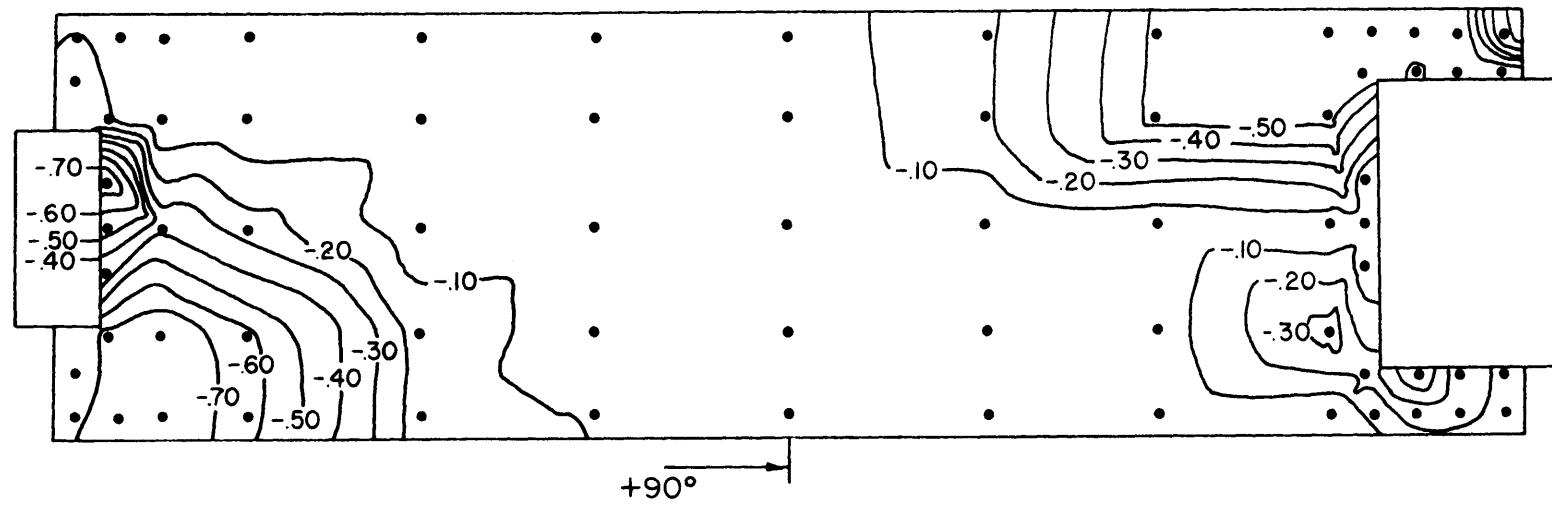
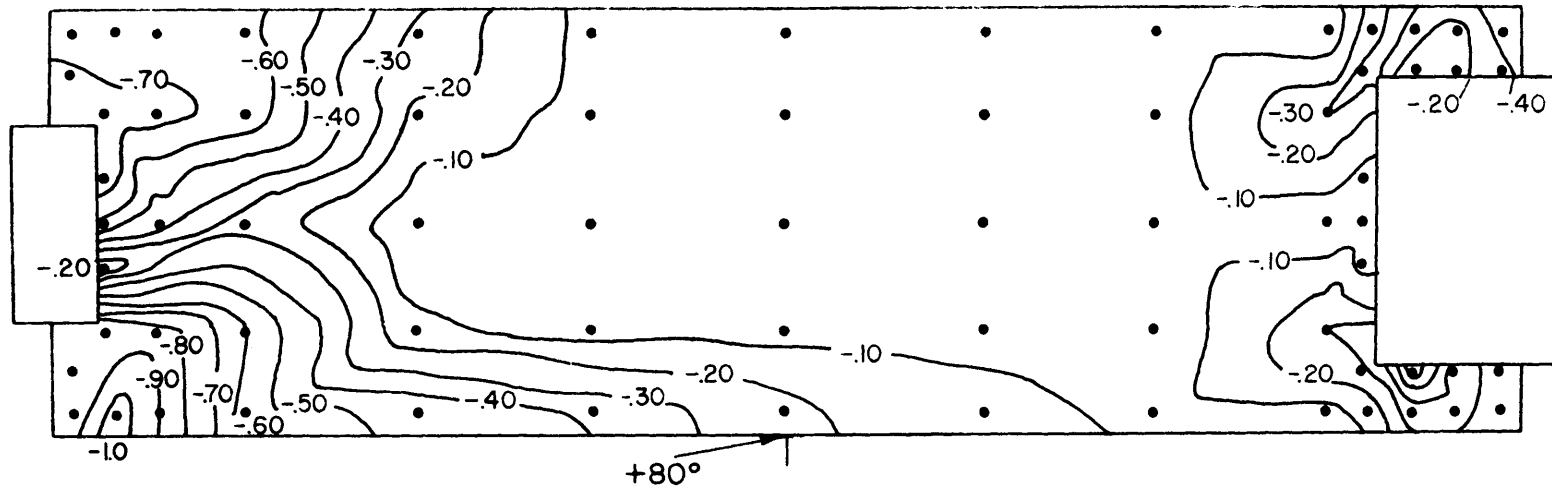


Fig. 22 Mean pressure coefficients for $\alpha = 80^\circ$ and 90° (Uniform Flow)

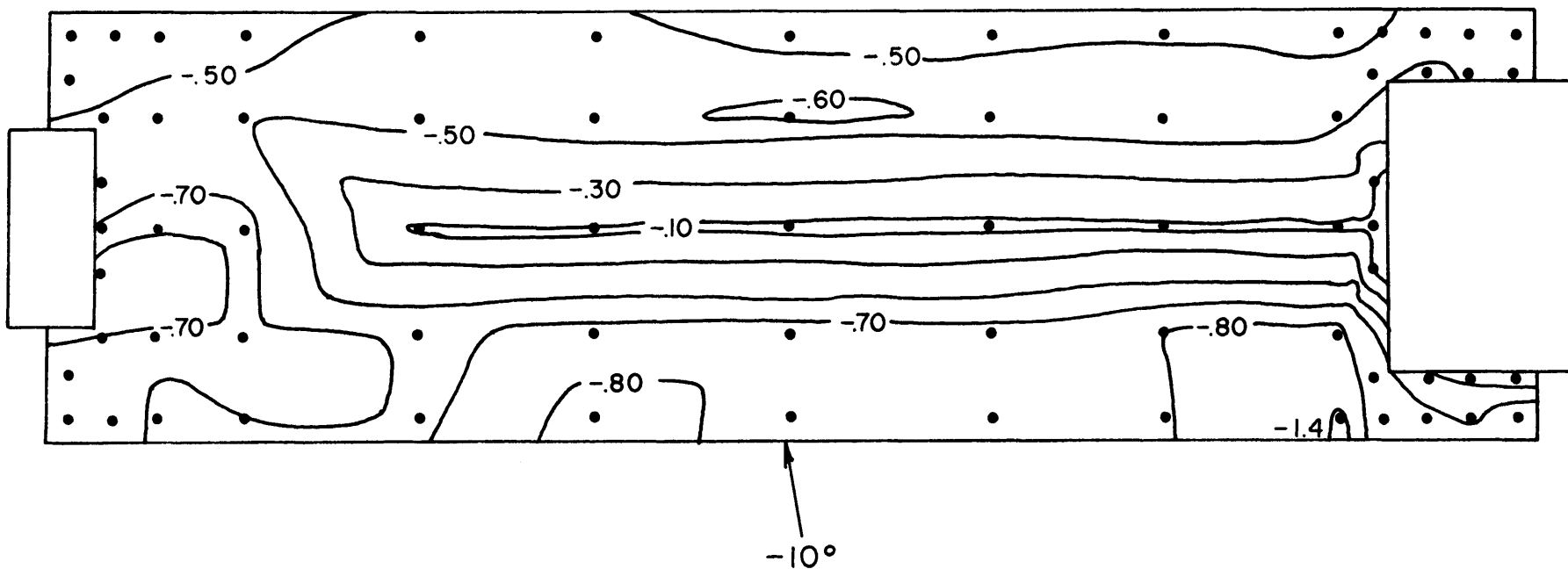


Fig. 23 Mean pressure coefficients for $\alpha = -10^\circ$ (Uniform Flow)

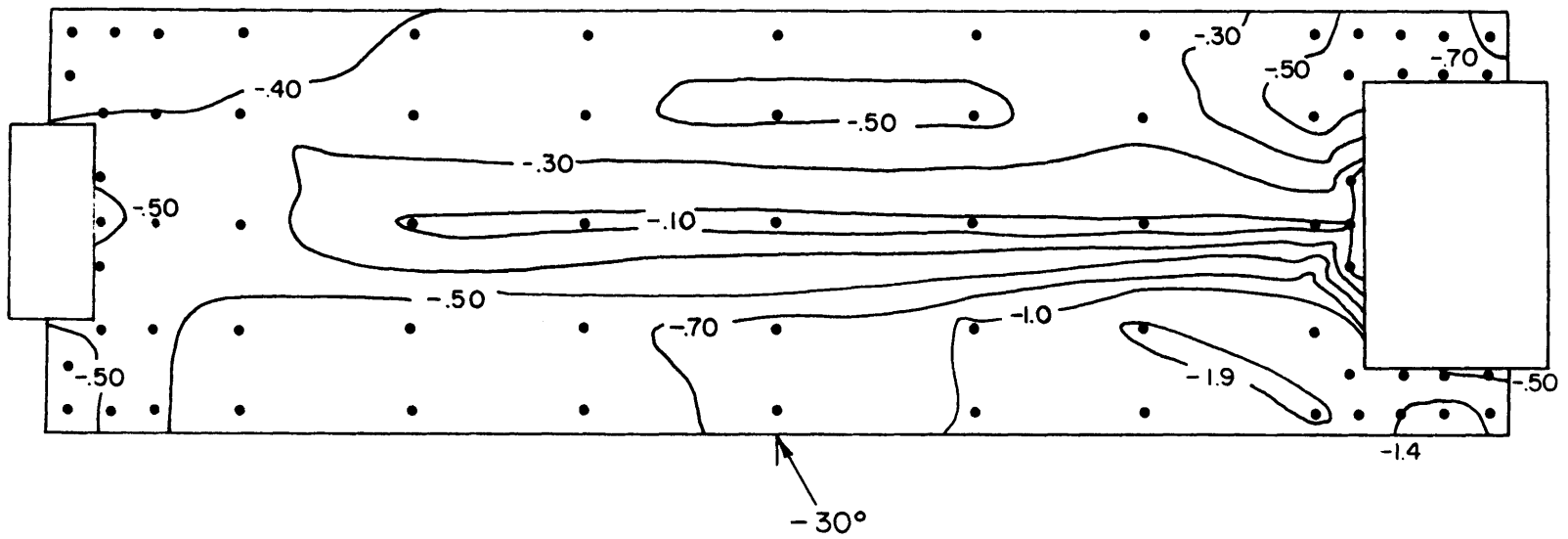
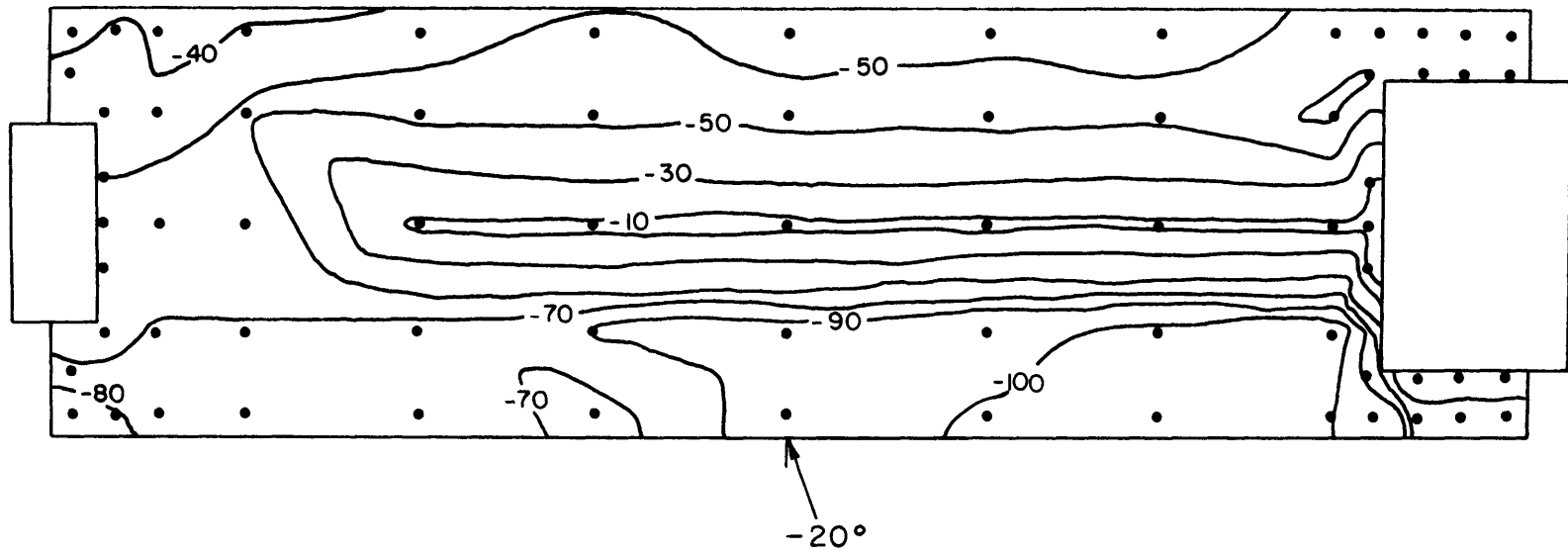


Fig. 24 Mean pressure coefficients for $\alpha = -20^\circ$ and -30° (Uniform Flow)

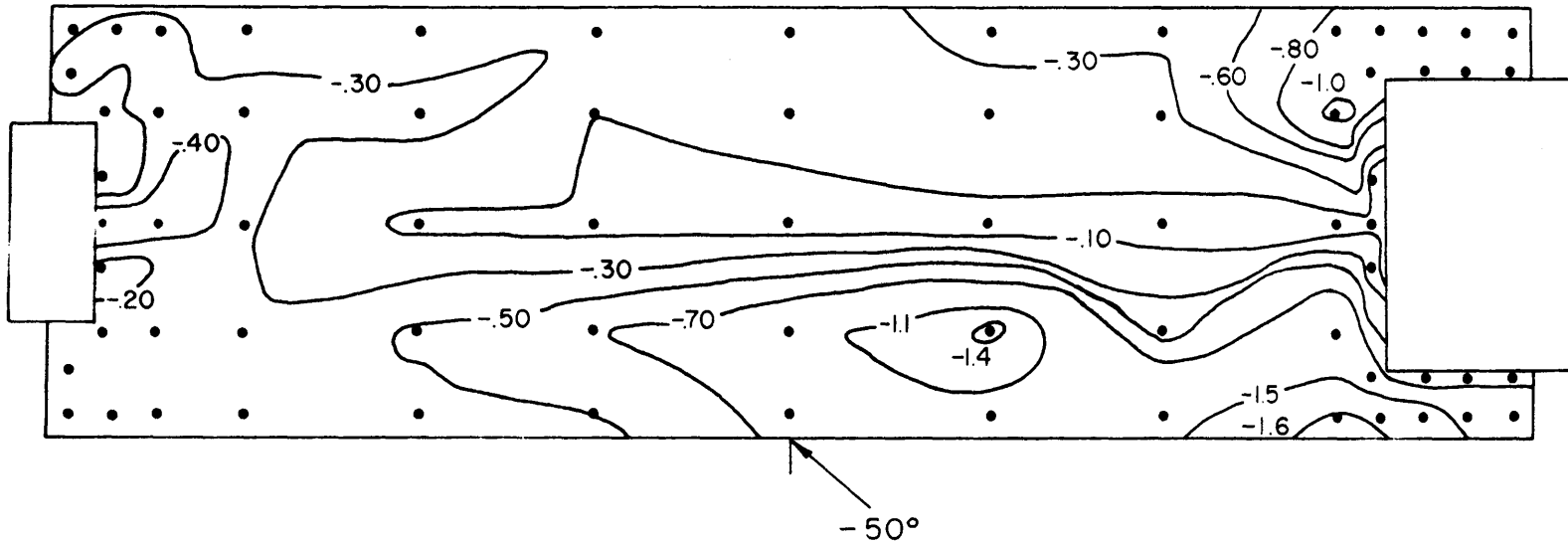
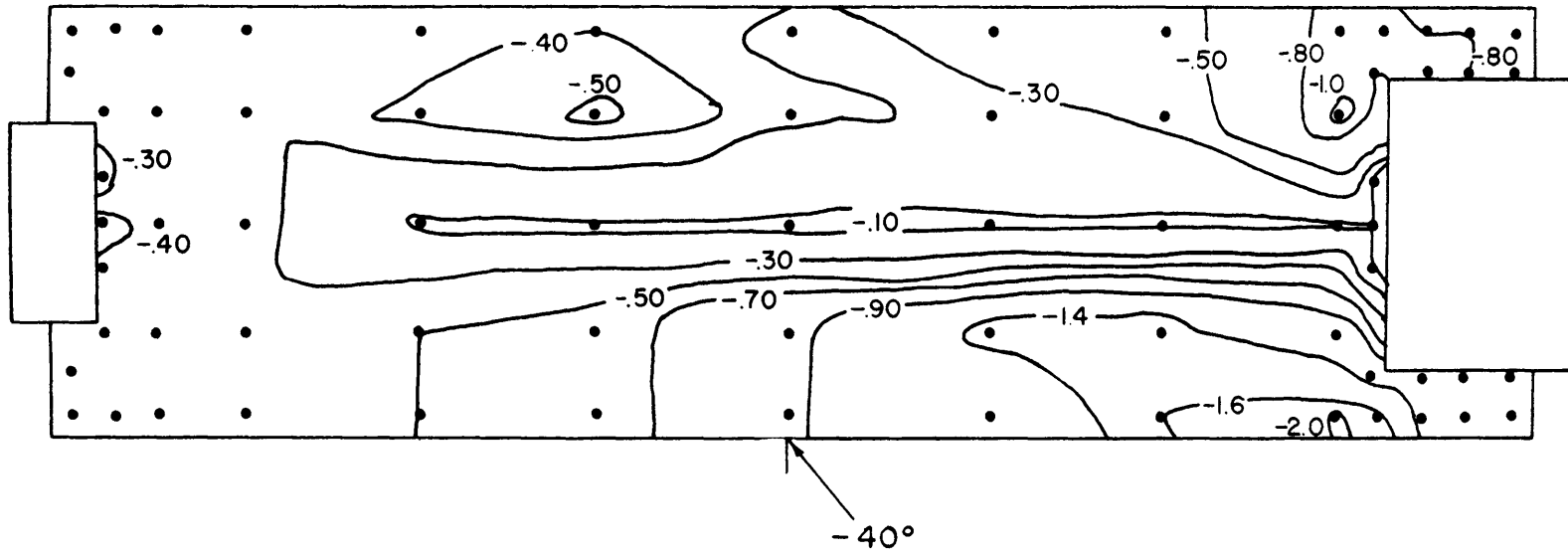


Fig. 25 Mean pressure coefficients for $\alpha = -40^\circ$ and -50° (Uniform Flow)

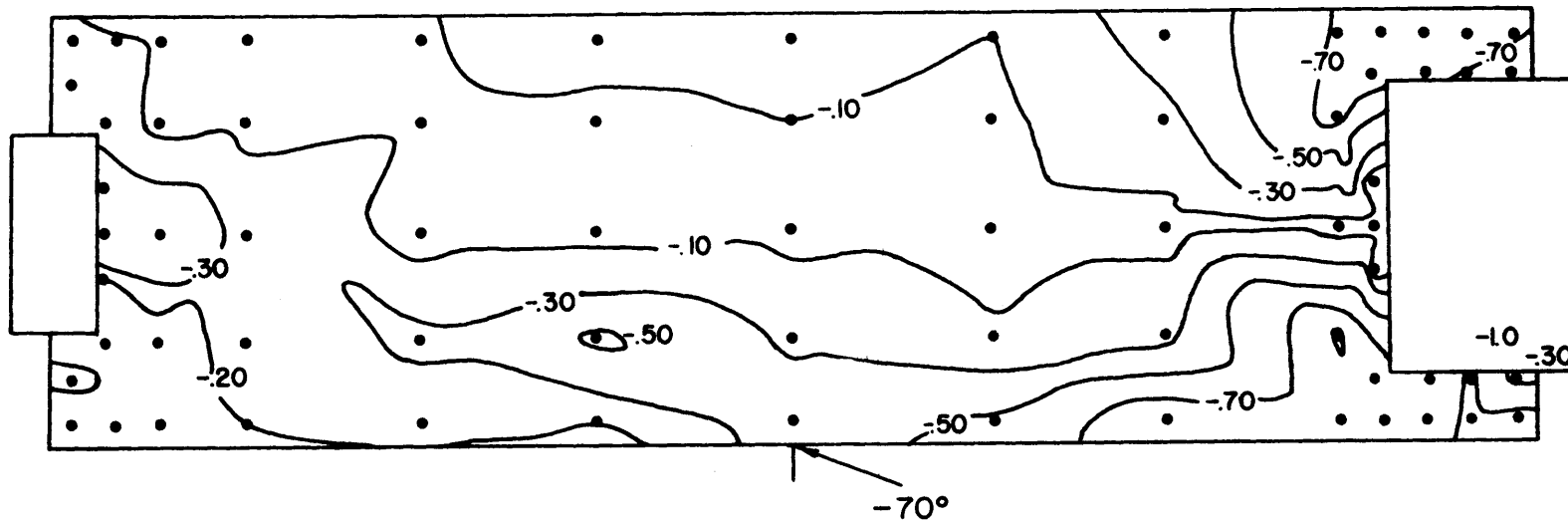
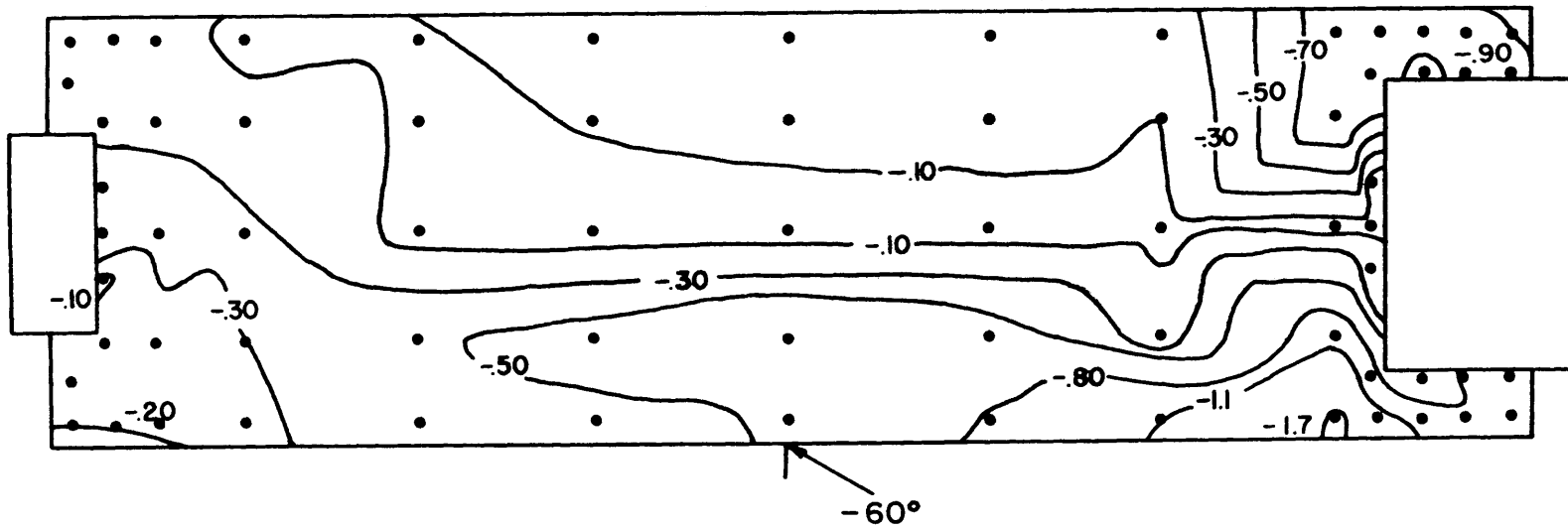


Fig. 26 Mean pressure coefficients for $\alpha = -60^\circ$ and -70° (Uniform Flow)

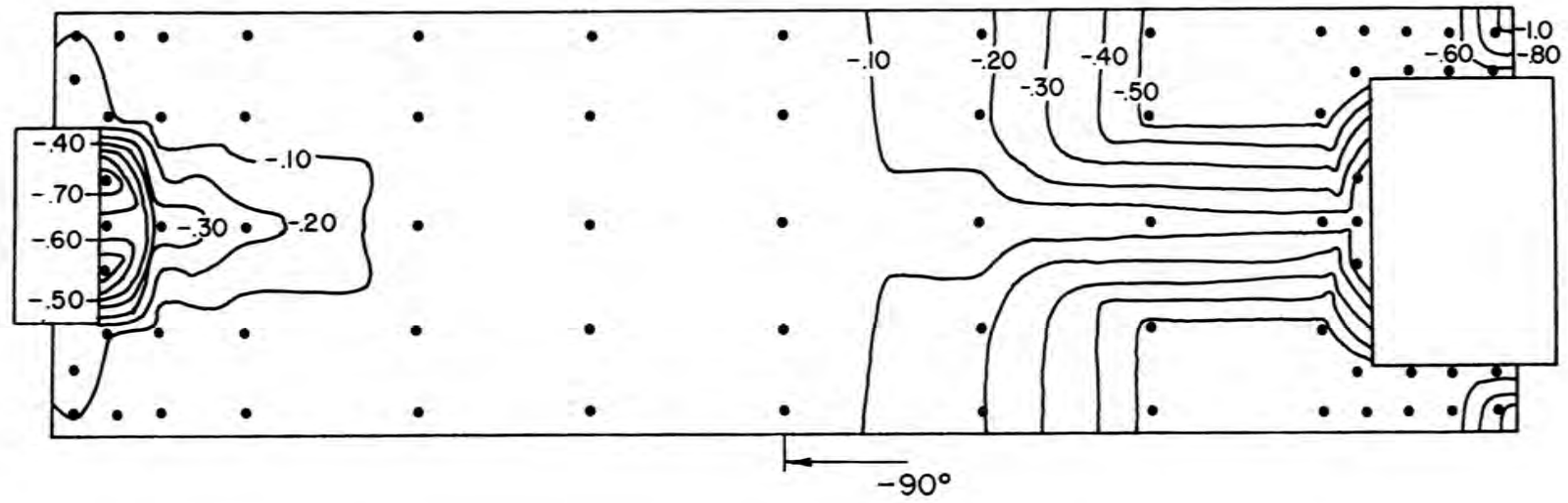
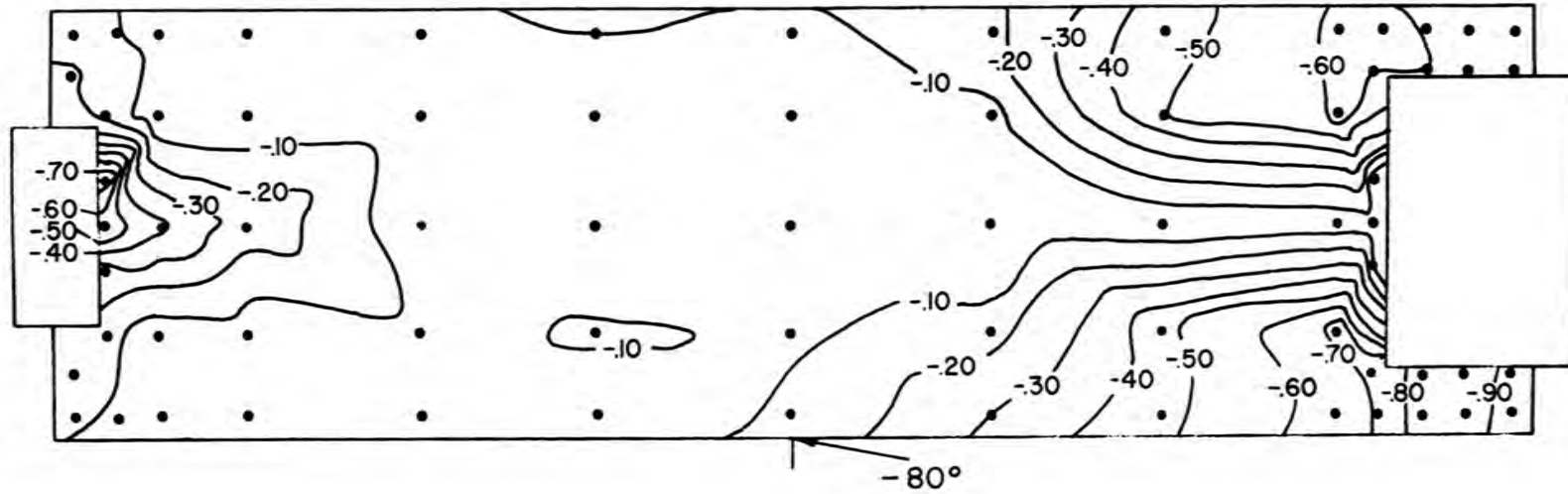


Fig. 27 Mean pressure coefficients for $\alpha = -80^\circ$ and -90° (Uniform Flow)

Drawings of isobars on roof of Building No. 226 measured as

$$C_p = \frac{P - P_{\text{ref}}}{\rho \bar{U}_{\text{ref}}^2 / 2}$$

For Boundary Layer Flow

Figs. 28-37

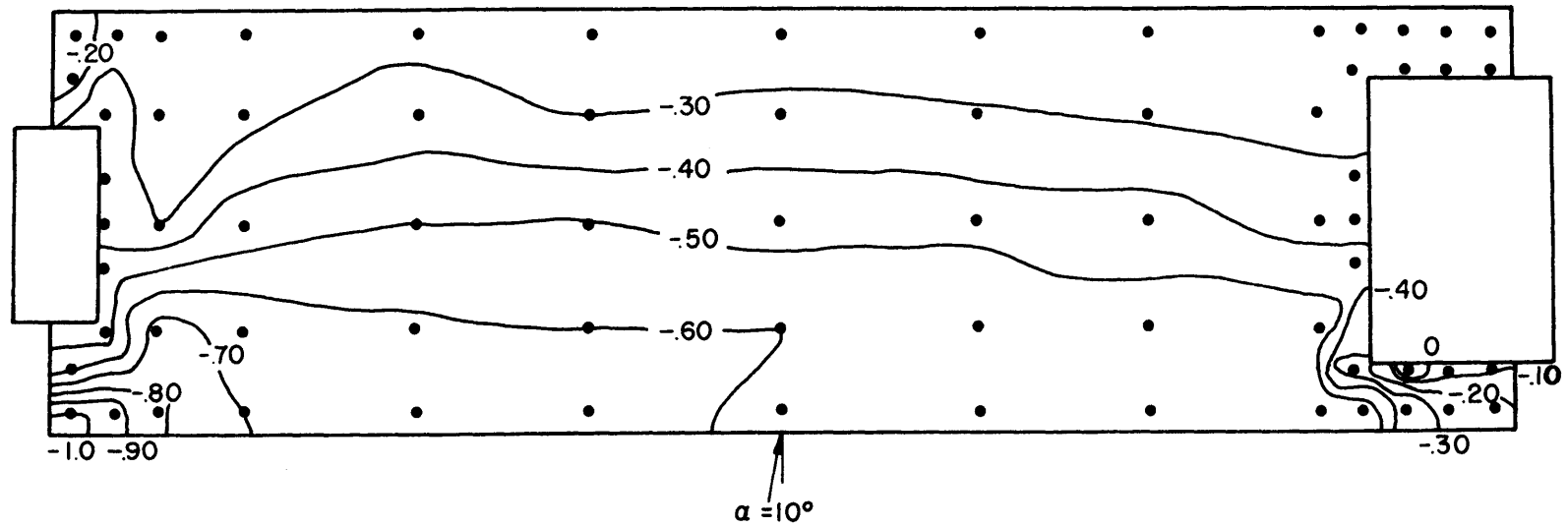
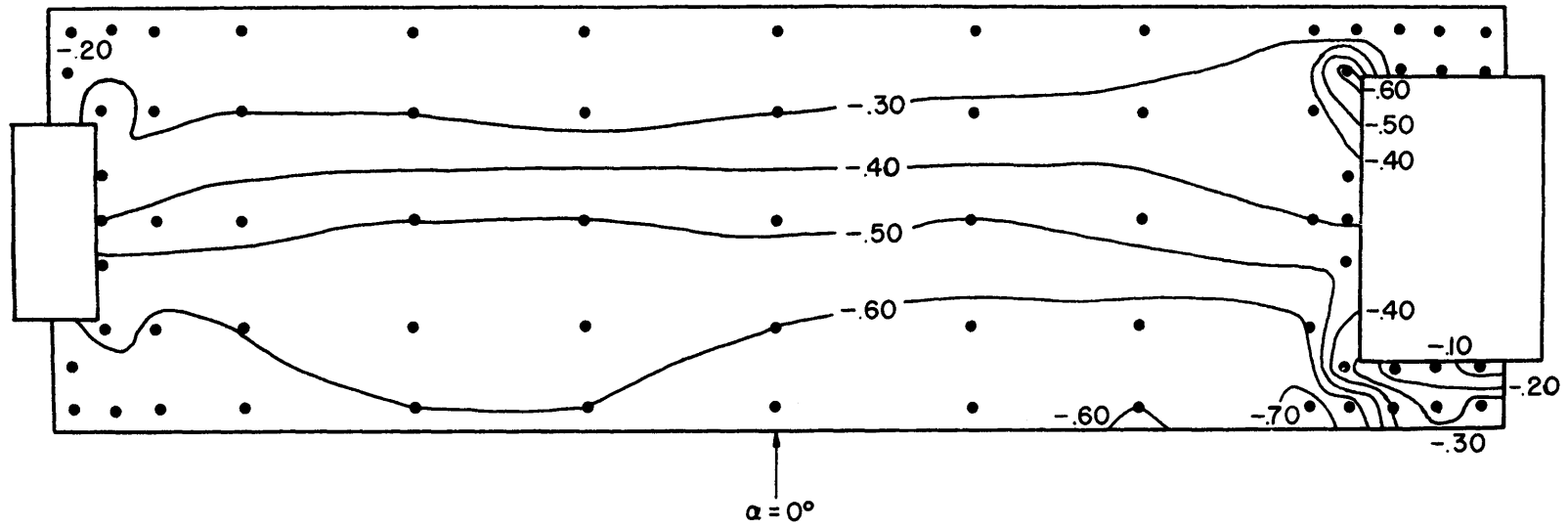


Fig. 28 Mean pressure coefficients for $\alpha = 0^\circ$ and 10° (Boundary Layer -- $\delta/H = 4.1$)

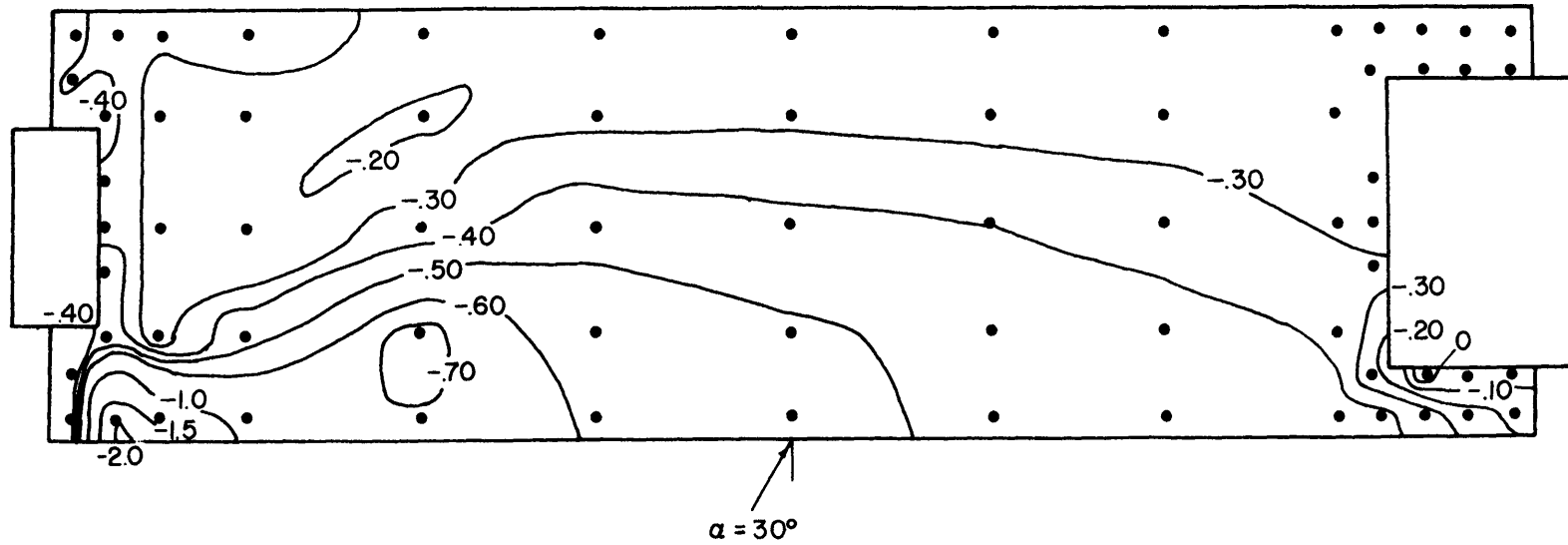
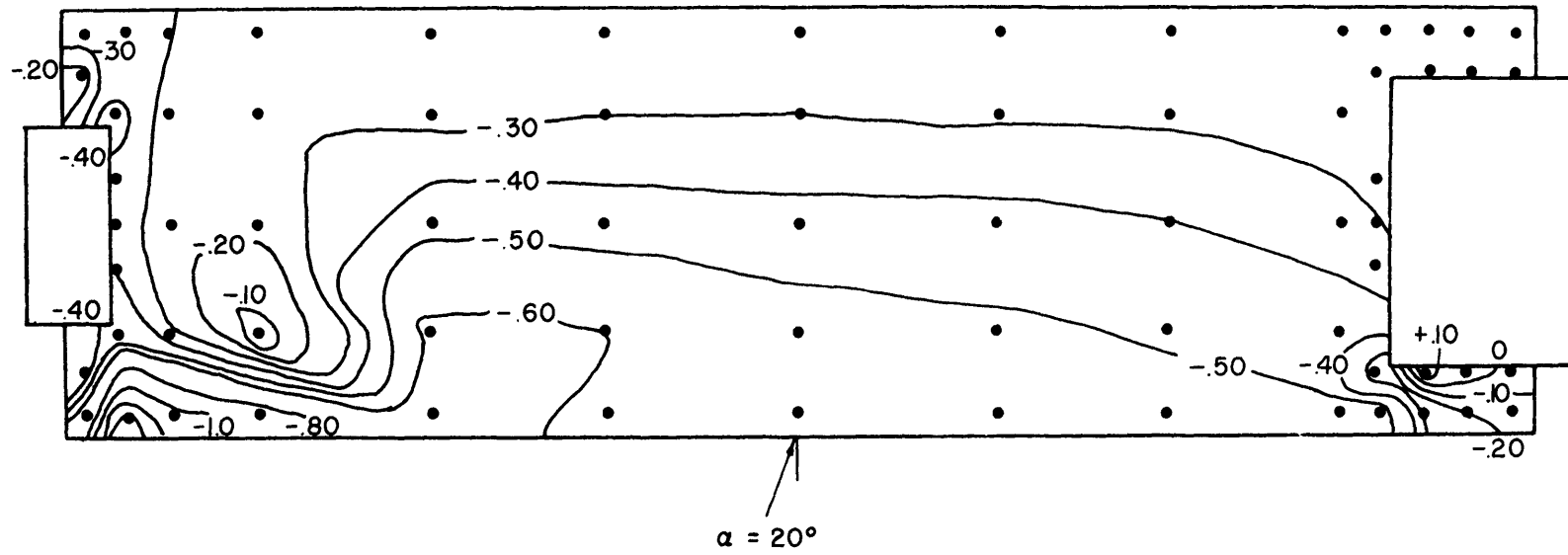


Fig. 29 Mean pressure coefficients for $\alpha = 20^\circ$ and 30° (Boundary Layer -- $\delta/H = 4.1$)

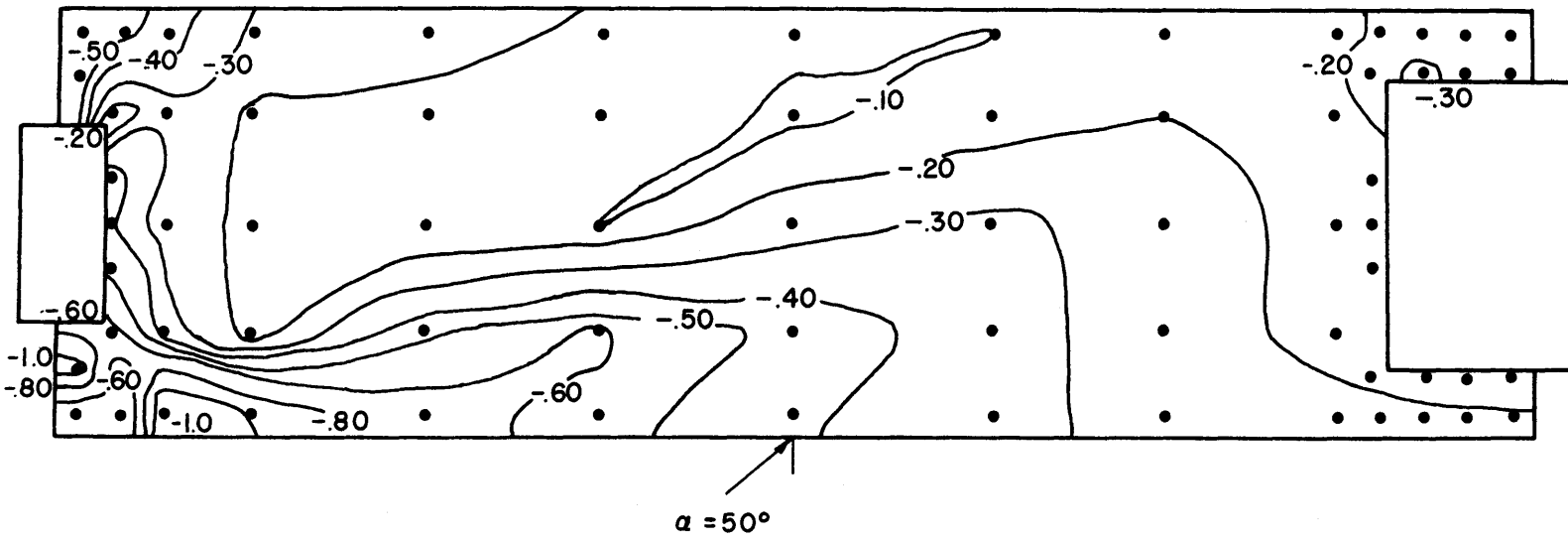
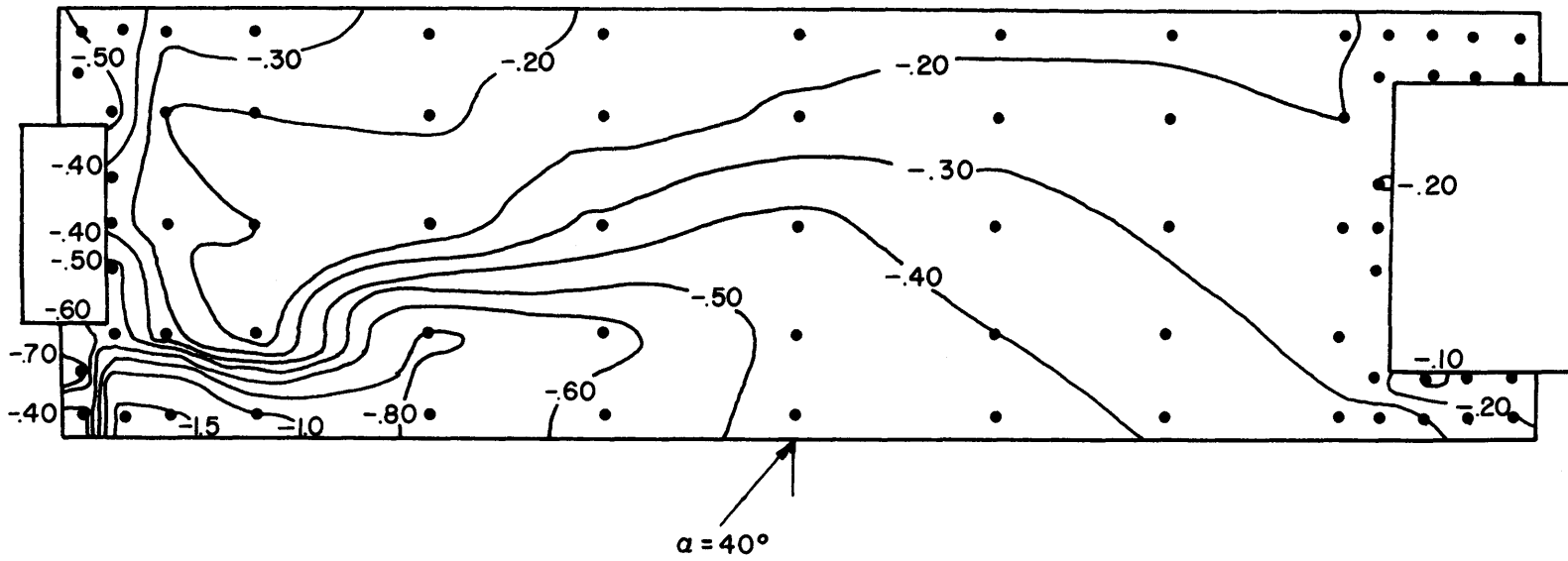


Fig. 30 Mean pressure coefficients for $\alpha = 40^\circ$ and 50° (Boundary Layer -- $\delta/H = 4.1$)

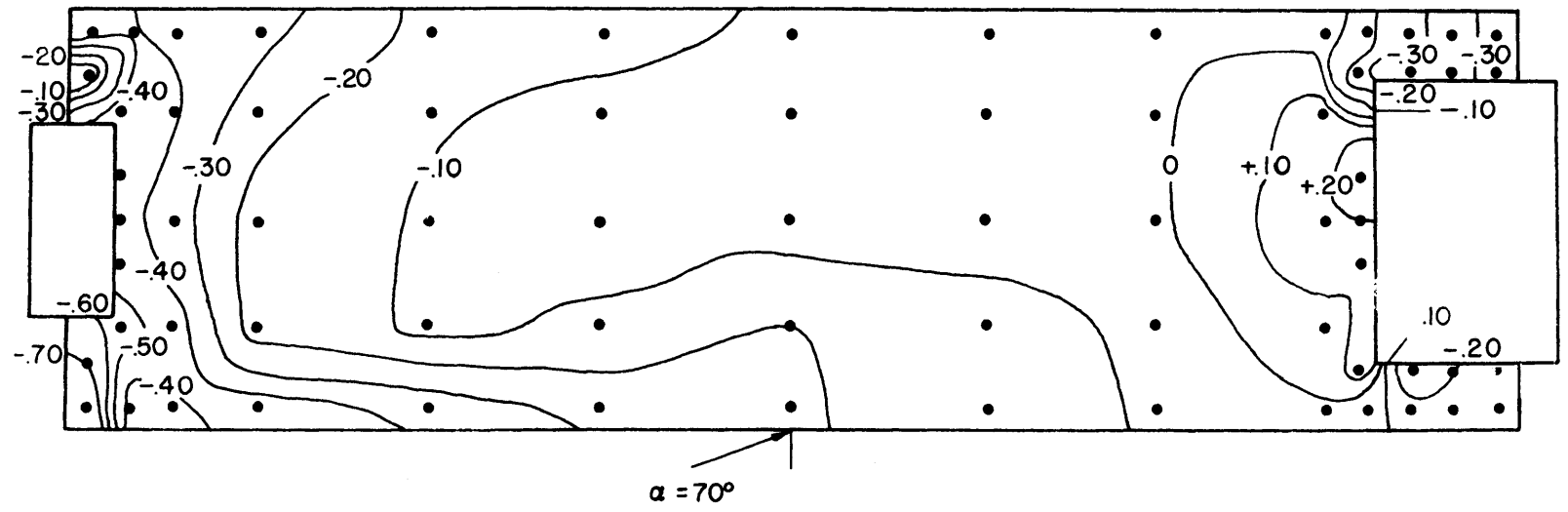
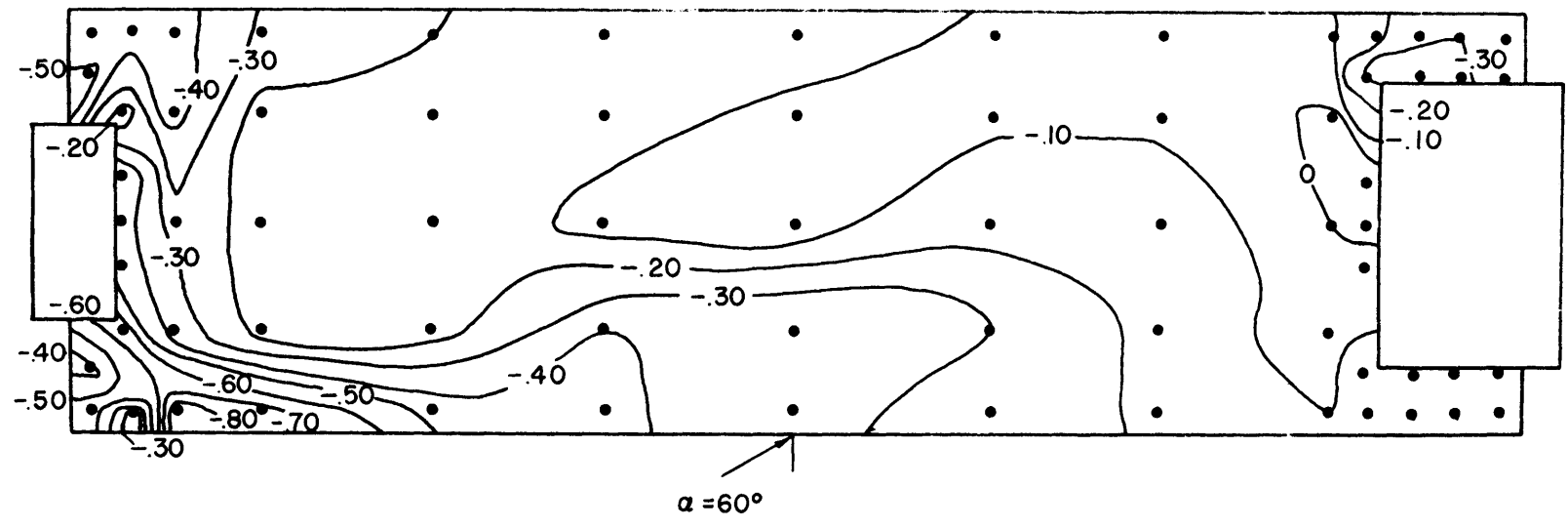


Fig. 31 Mean pressure coefficients for $\alpha = 60^\circ$ and 70° (Boundary Layer -- $\delta/H = 4.1$)

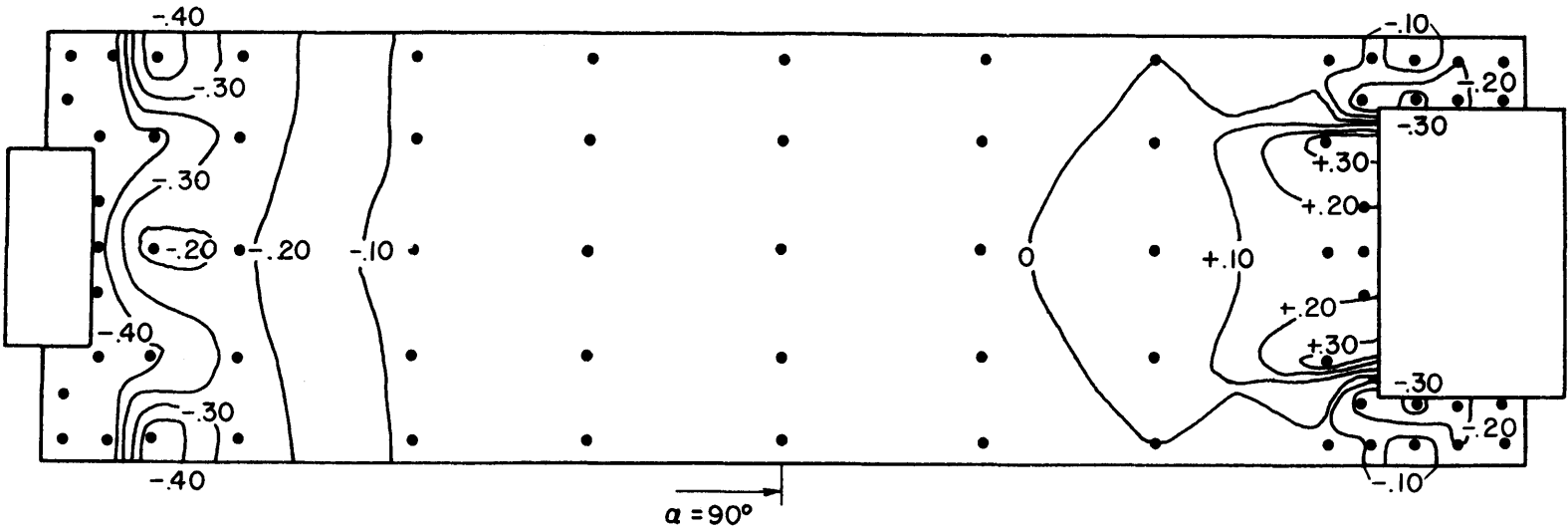
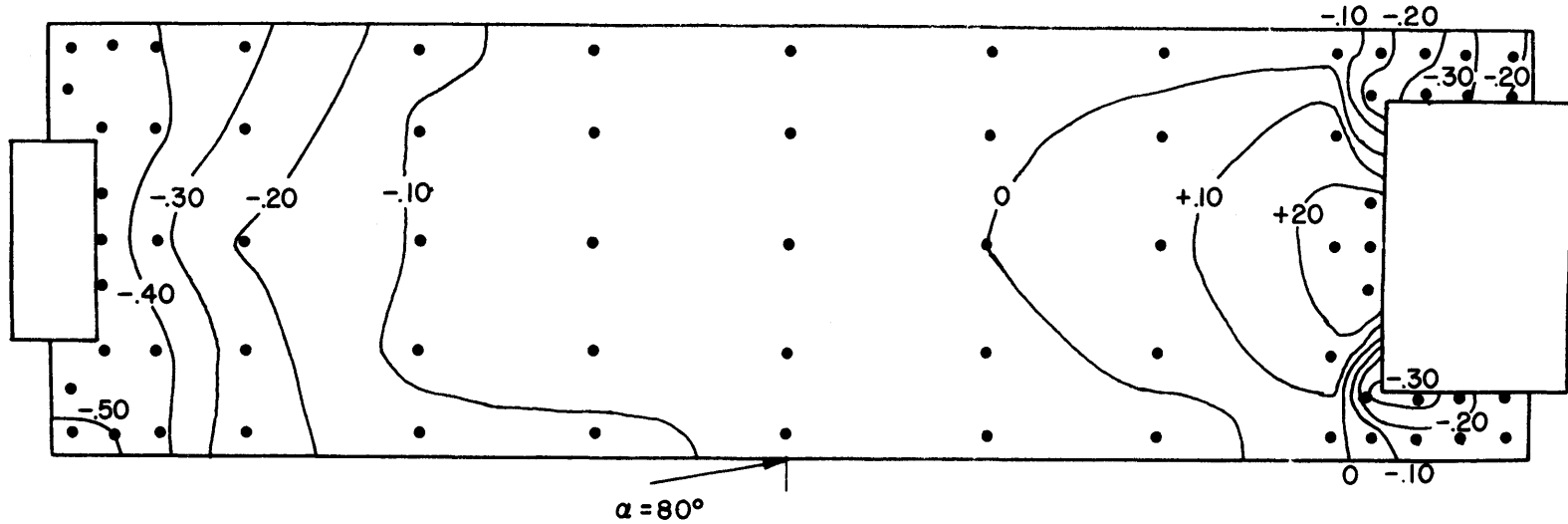


Fig. 32 Mean pressure coefficients for $\alpha = 80^\circ$ and 90° (Boundary Layer -- $\delta/H = 4.1$)

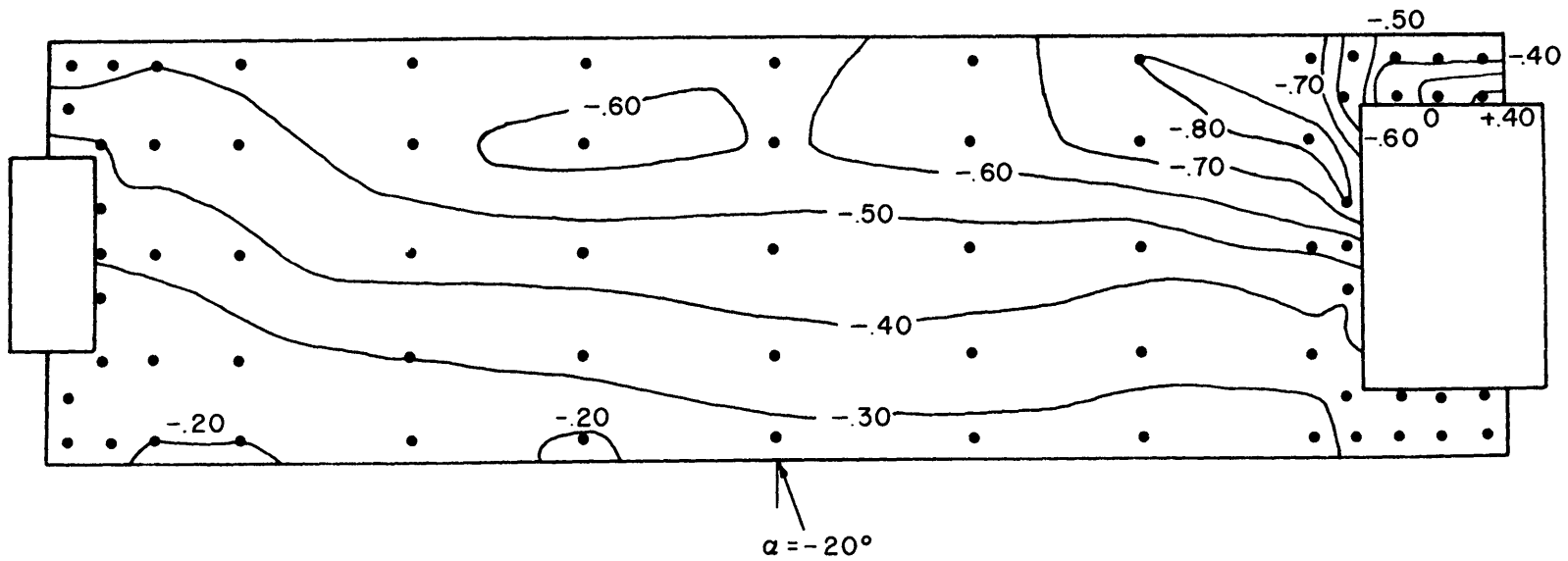
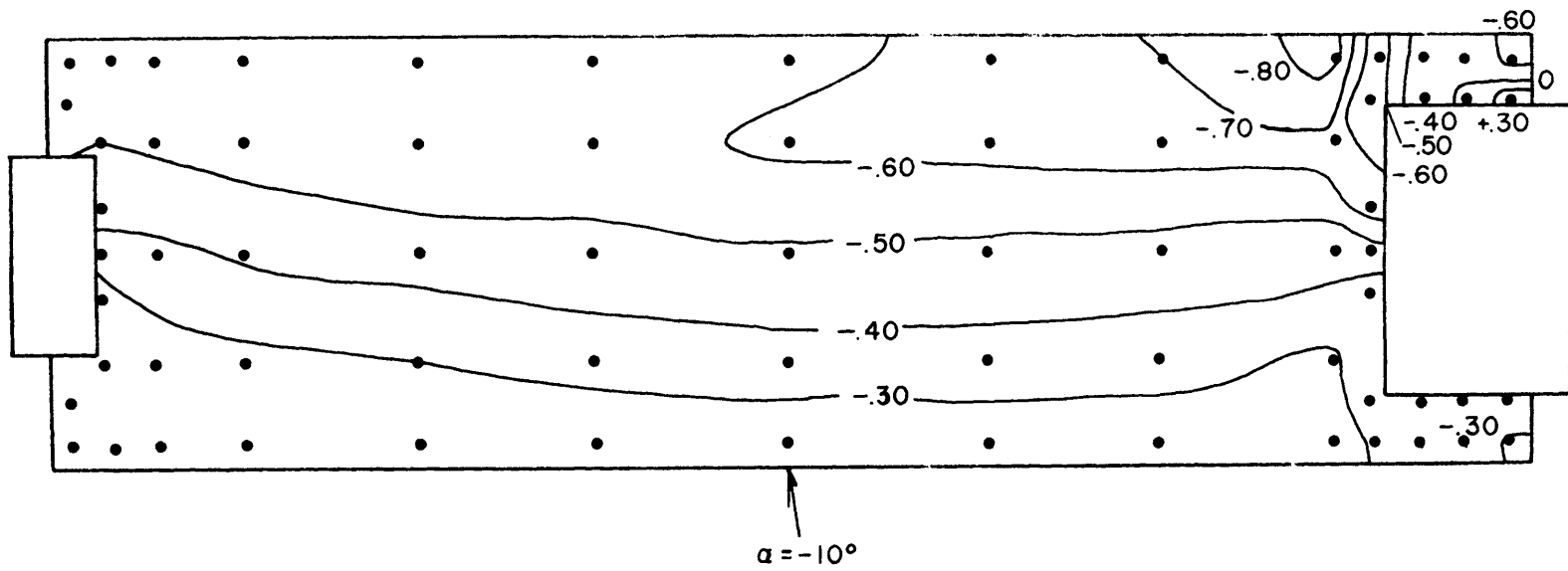


Fig. 33 Mean pressure coefficients for $\alpha = -10^\circ$ and -20° (Boundary Layer -- $\delta/l = 4.1$)

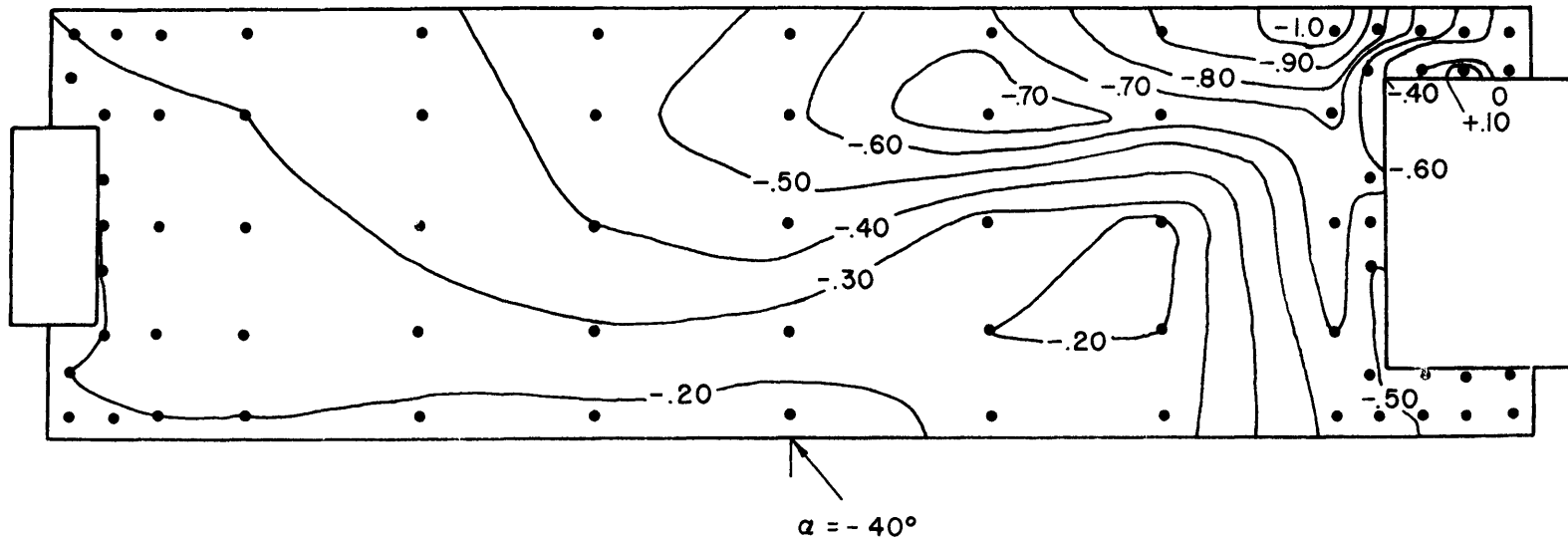
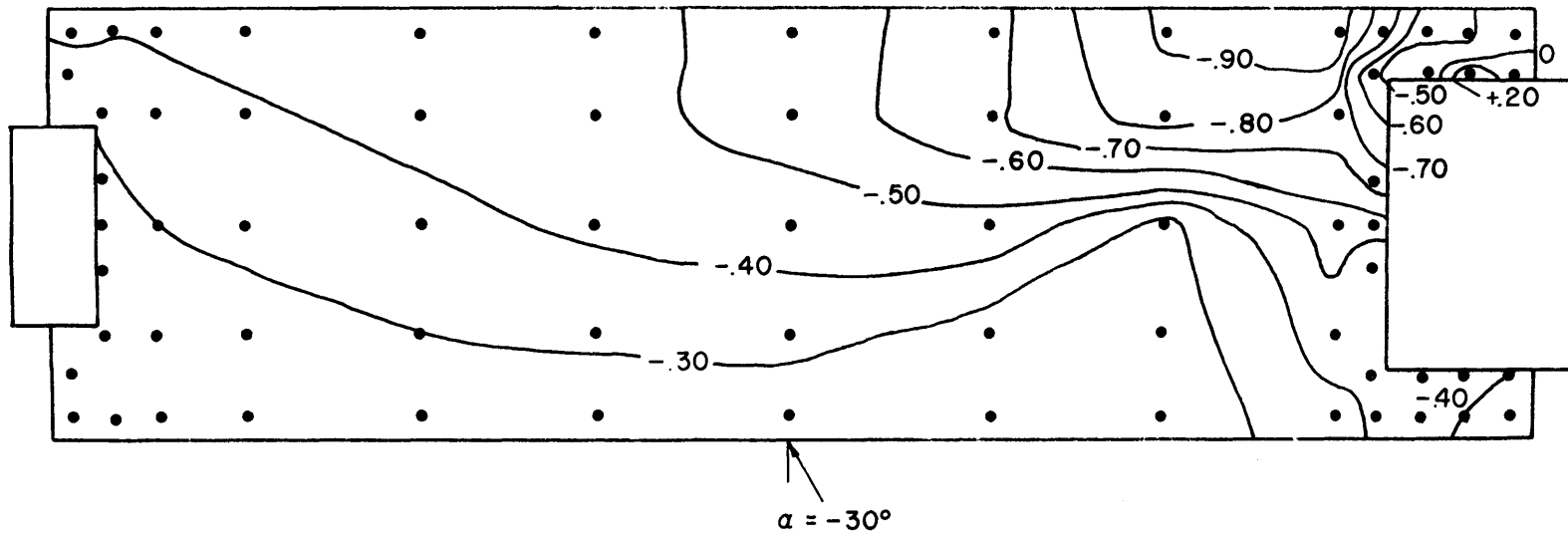


Fig. 34 Mean pressure coefficients for $\alpha = -30^\circ$ and -40° (Boundary Layer -- $\delta/H = 4.1$)

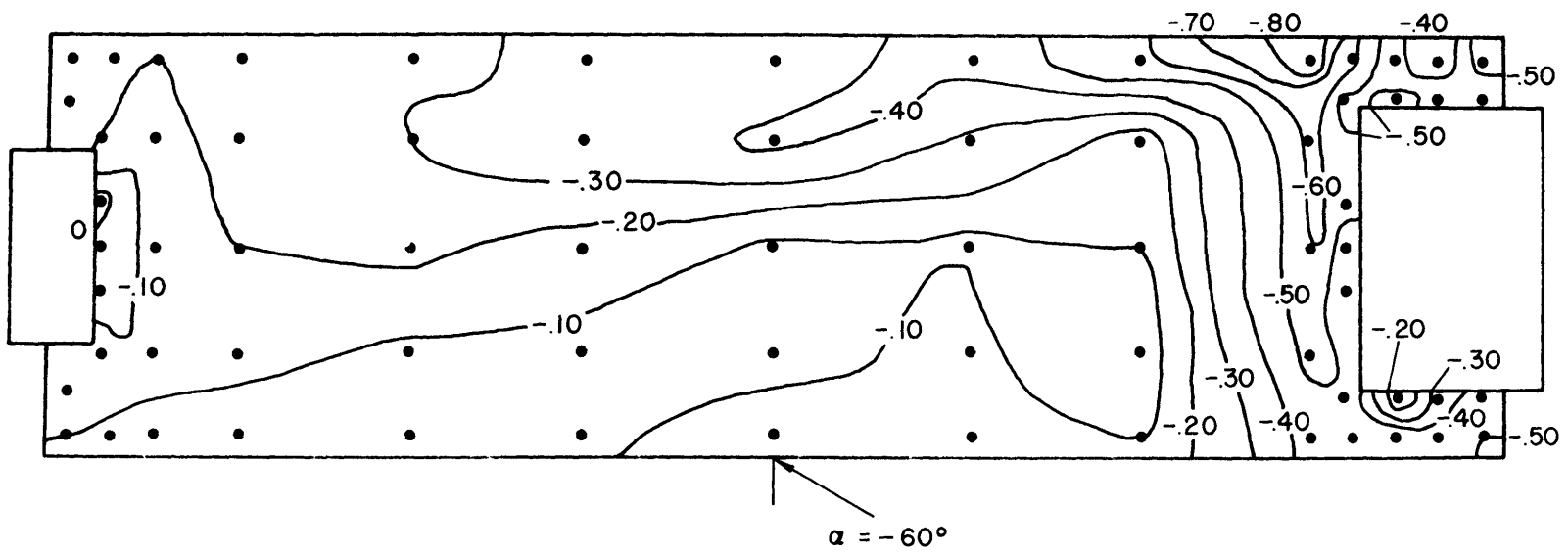
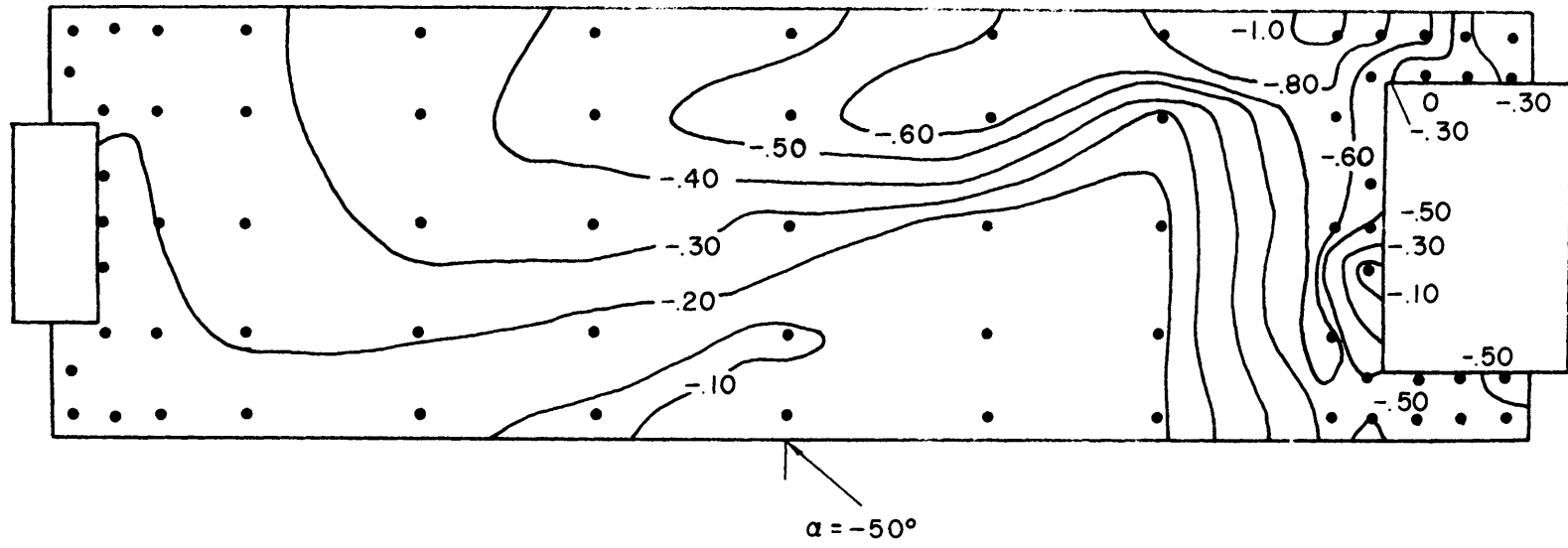


Fig. 35 Mean pressure coefficients for $\alpha = -50^\circ$ and -60° (Boundary Layer -- $\delta/H = 4.1$)

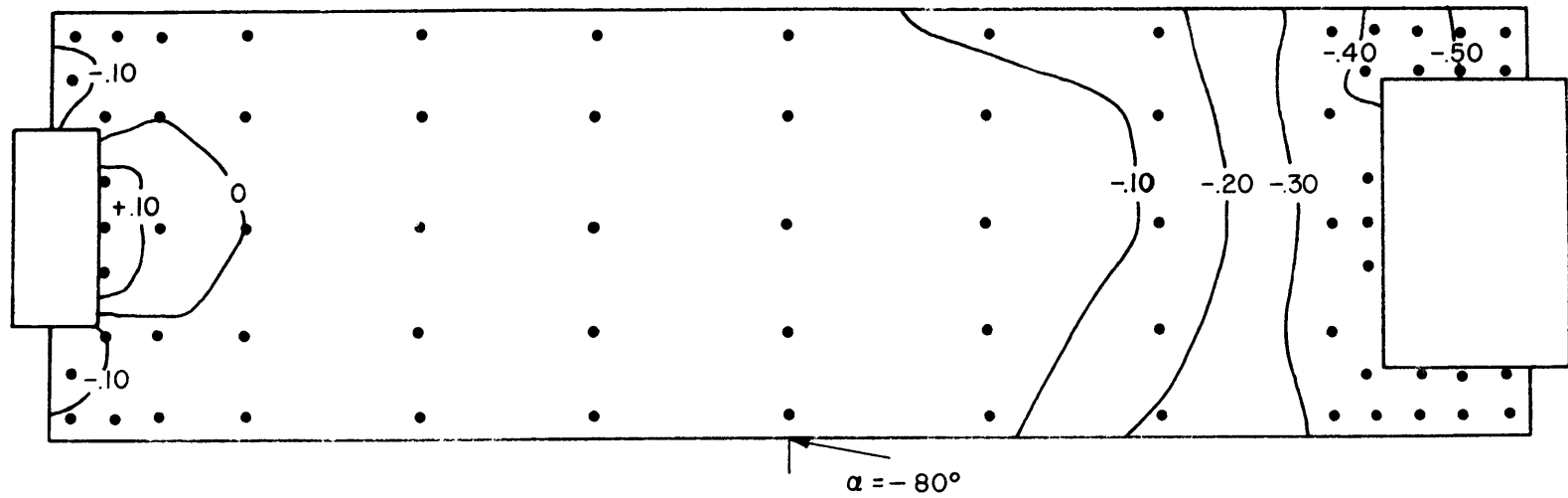
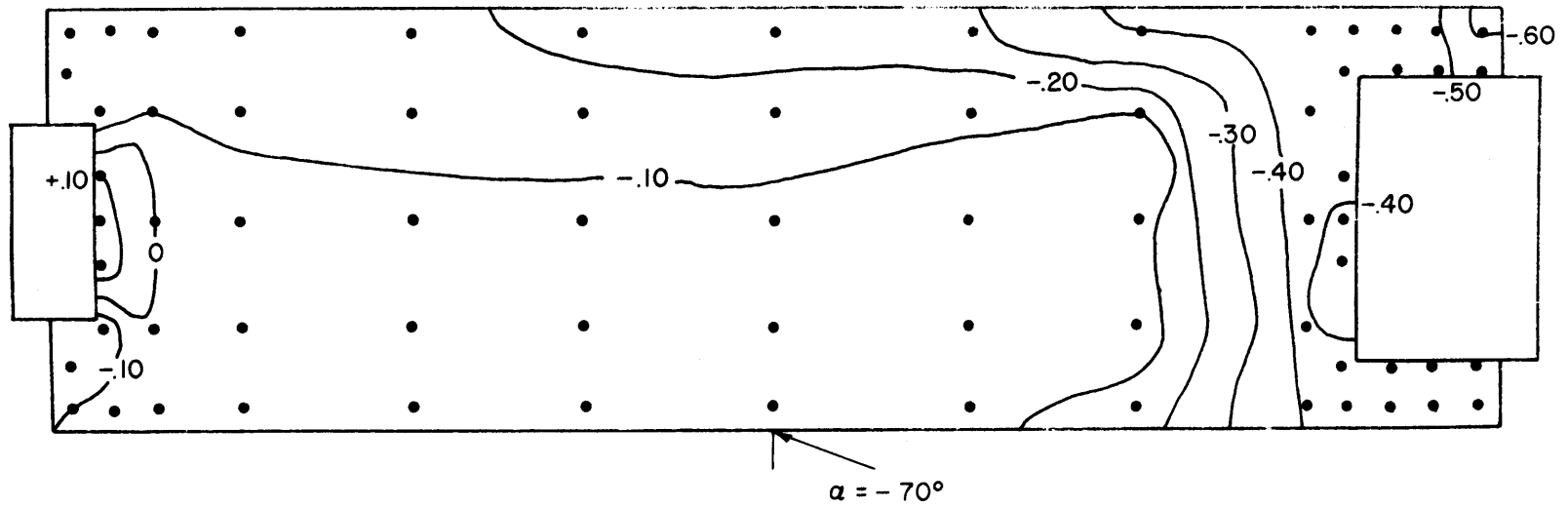


Fig. 36 Mean pressure coefficients for $\alpha = -70^\circ$ and -80° (Boundary Layer -- $\delta/H = 4.1$)

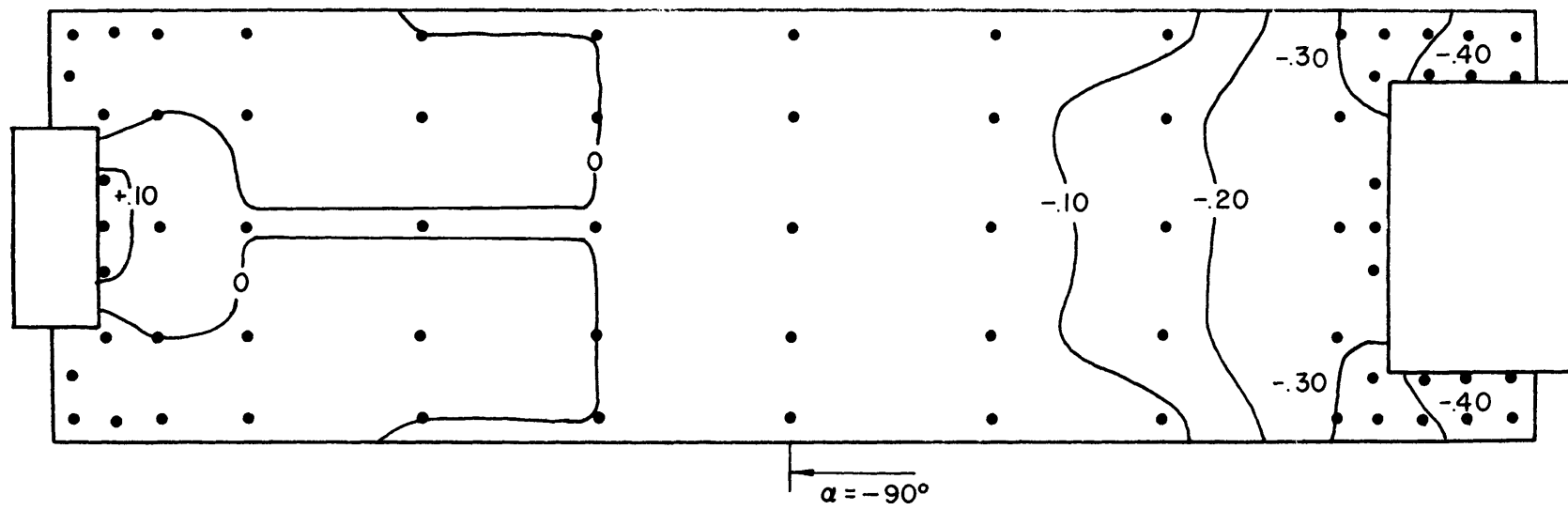


Fig. 37 Mean pressure coefficients for $\alpha = -90^\circ$ (Boundary Layer -- $\delta/H = 4.1$)

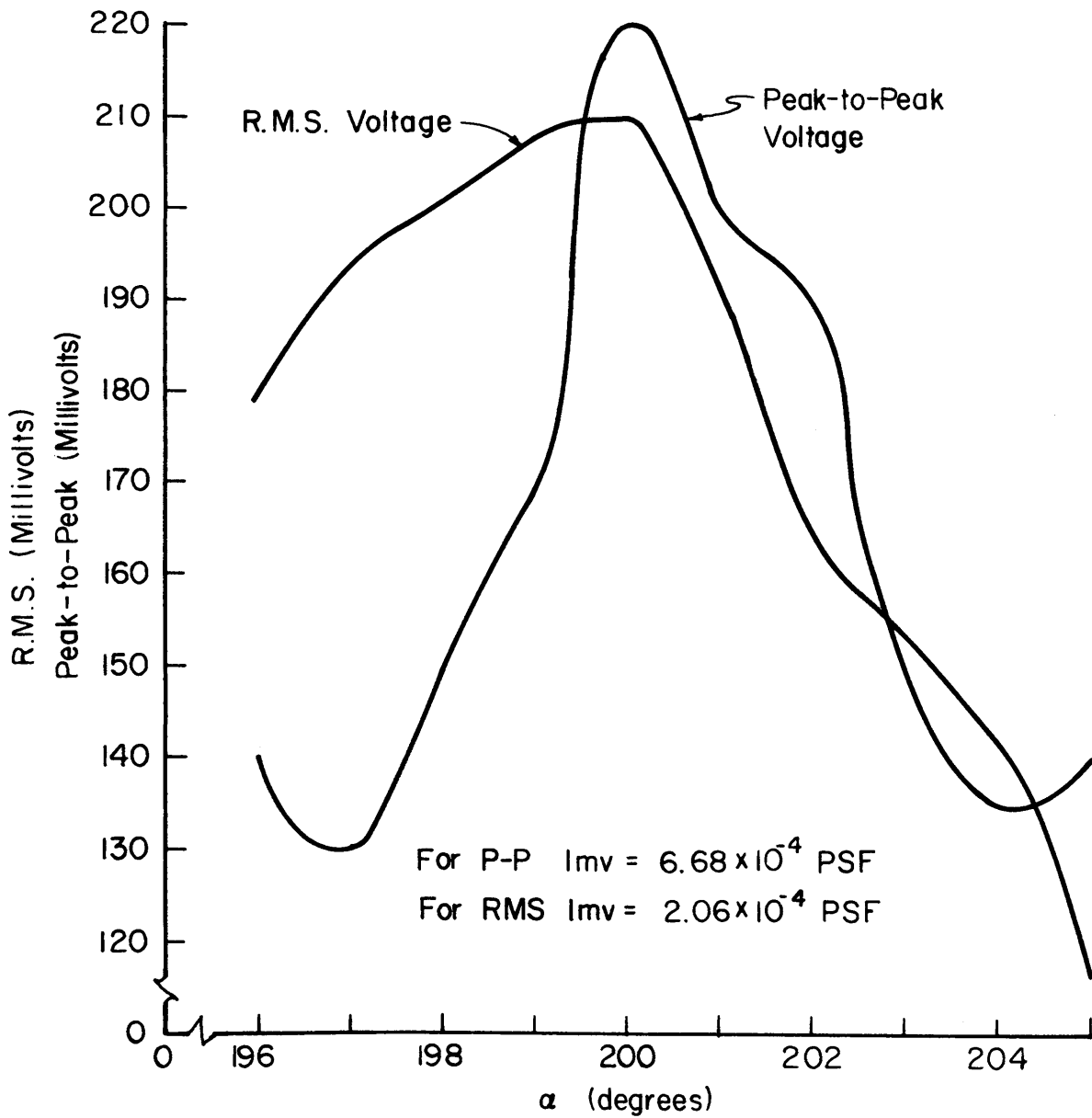


Fig. 38 Angle-of-attack vs transducer RMS and peak-to-peak output

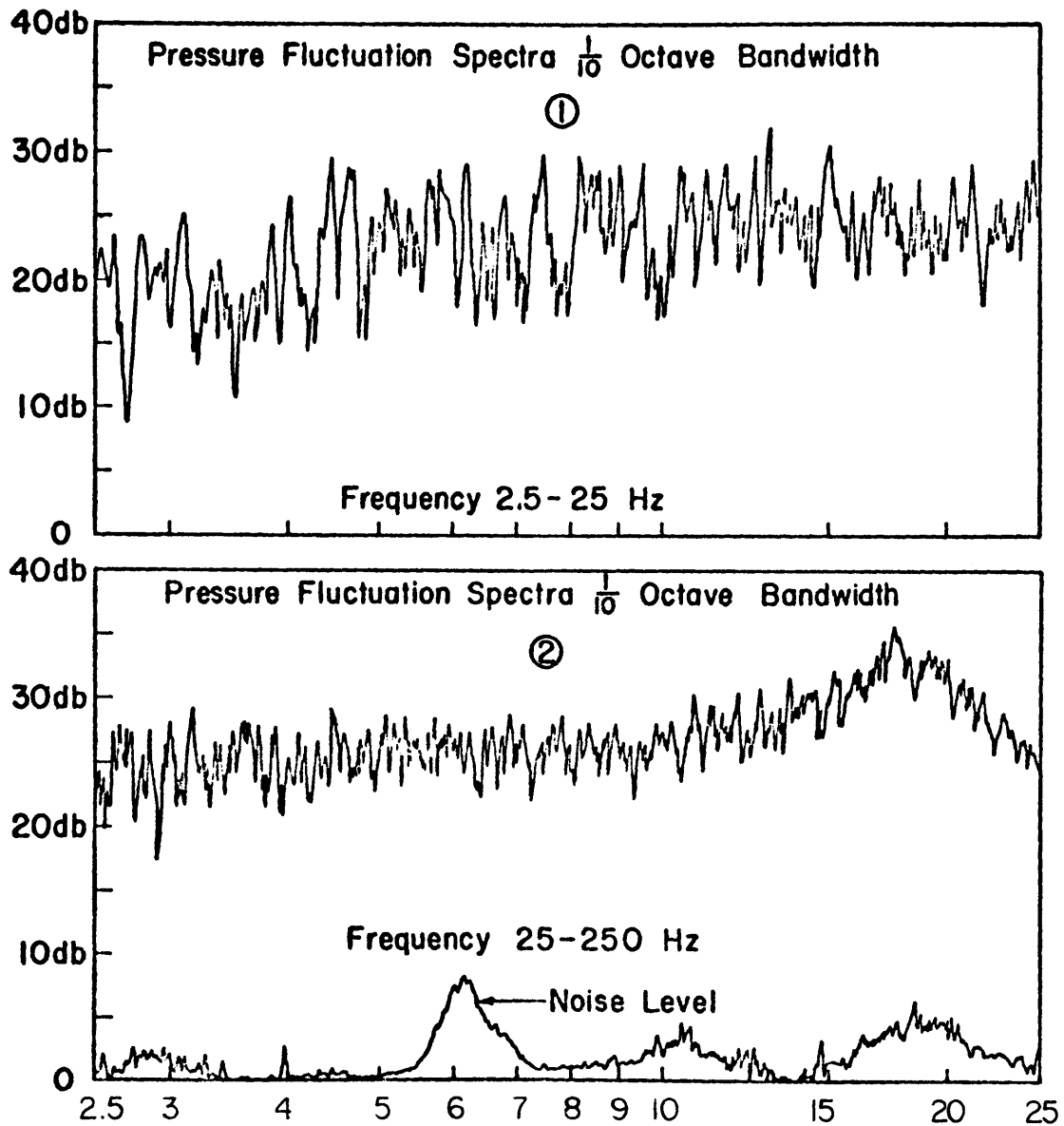


Fig. 39 Typical output from wave analyzer for $\bar{U}_{ref} = 26.2$ ft/sec.

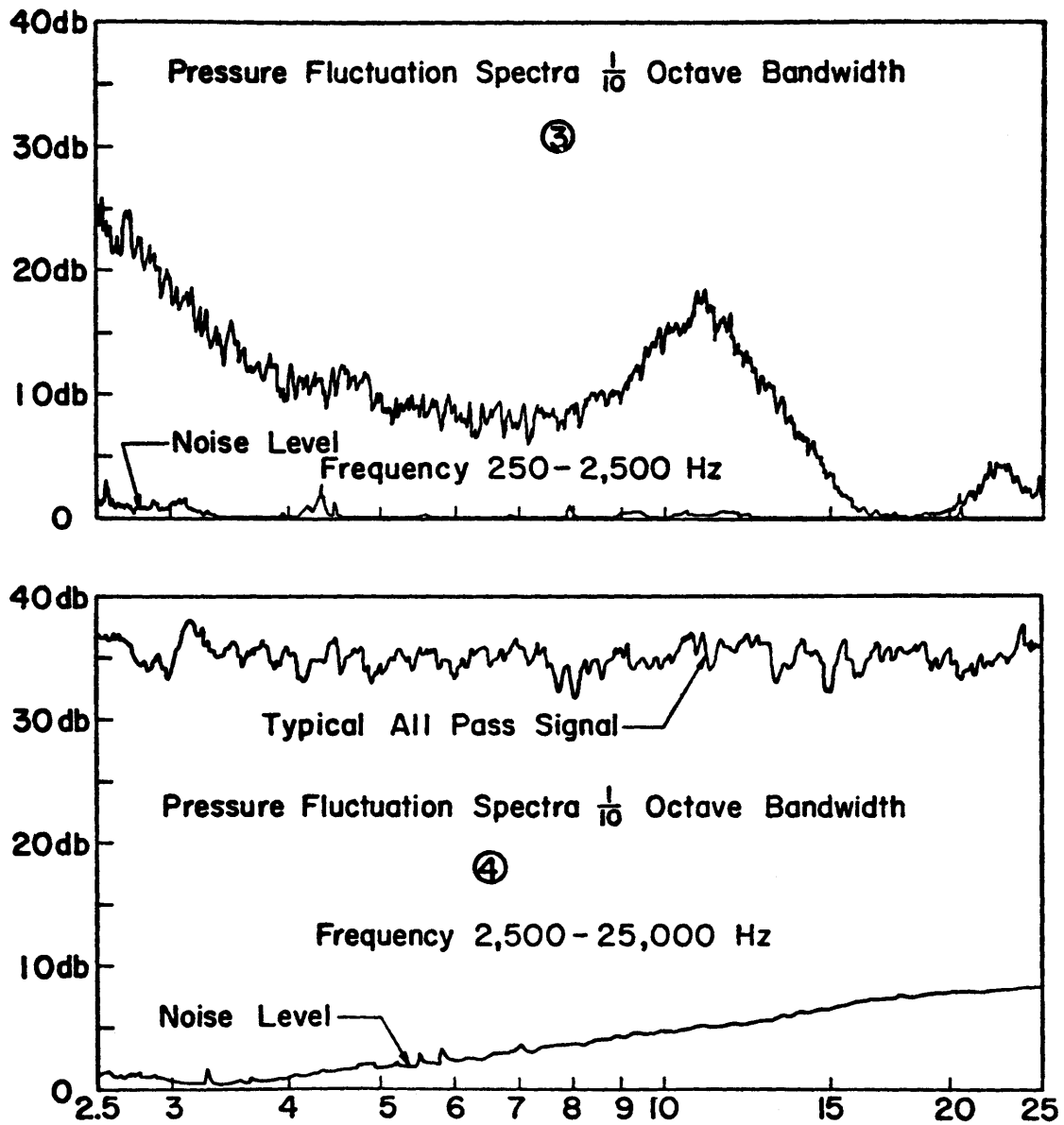


Fig. 39a Typical output from wave analyzer for $\bar{U}_{ref} = 26.2$ ft/sec.

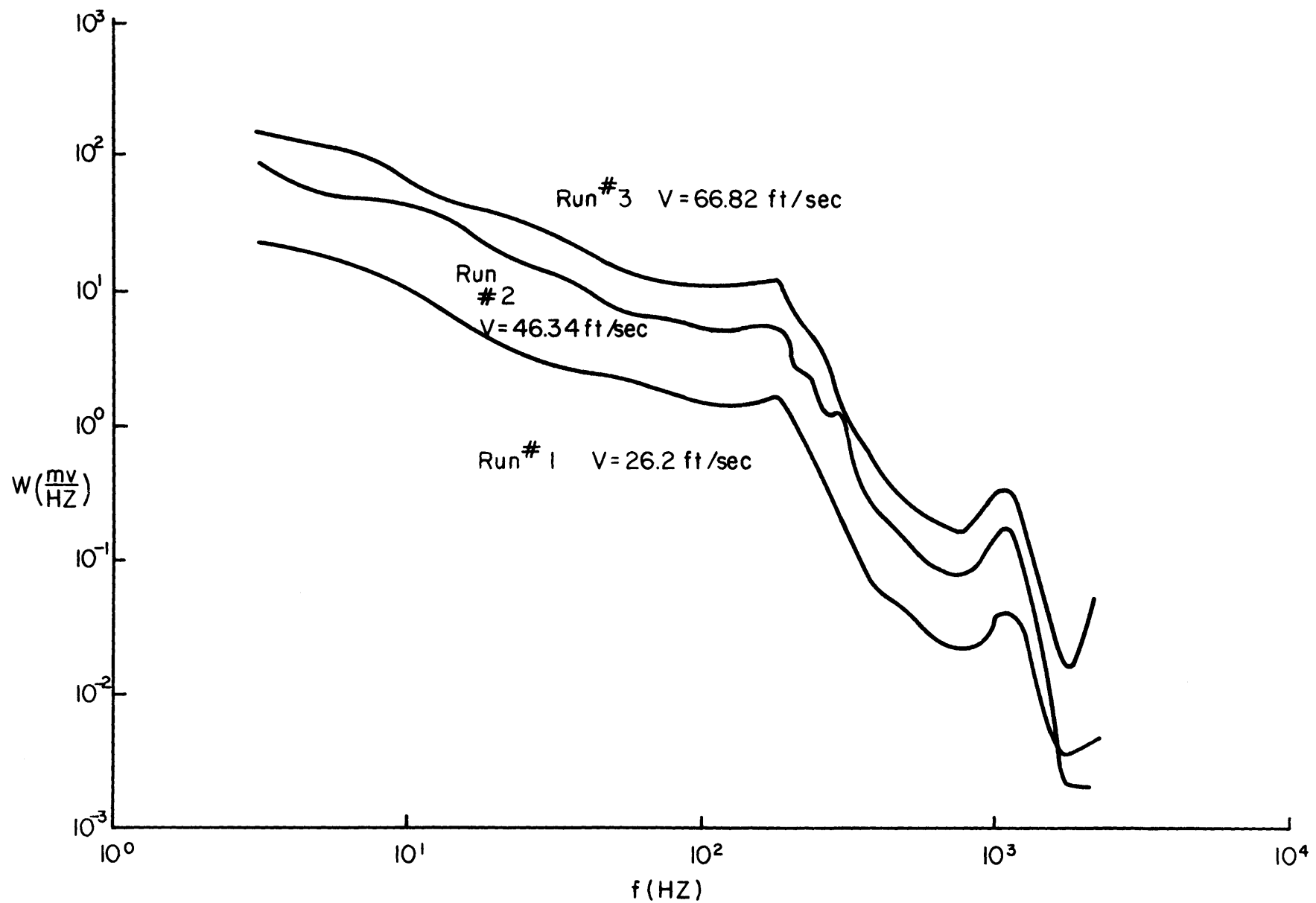


Fig. 40 Pressure-fluctuation spectra for pressure tap No. 1 at $\alpha = 200^\circ$